NASA CONTRACTOR REPORT 166424

(NASA-CR-166424) EVALUATION OF THE EFFECT OF VIBRATION NONLINEARITY ON CONVERGENCE BEHAVIOR OF ADAPTIVE HIGHER HARMONIC CONTROLLERS (Connecticut Univ.) 51 p HC A04/MF A01 CSCL 01C G3/05

N83-18718

Unclas 08911

Evaluation of the Effect of Vibration Nonlinearity On Convergence Behavior of Adaptive Higher Harmonic Controllers

J. A. Molusis
P. Mookerjee
Y. Bar-Shalom

GRANT NAG 2-72
January 1983

NASA

NASA CONTRACTOR REPORT 166424

Evaluation of the Effect of Vibration Nonlinearity On Convergence Behavior of Adaptive Higher Harmonic Controllers

John A. Molusis
Purusottam Mookerjee
Yaakov Bar-Shalom
University of Connecticut
Storrs, Connecticut

Prepared for
Ames Research Center
under Grant NAG 2-72

National Aeronautics and
Space Administration

Ames Research Center
Moffett Field, California 94035

CONTENTS

SUMMARY

An evaluation of the effect of nonlinearity on convergence of the local linear and global linear adaptive controllers is presented. A nonlinear helicopter vibration model is selected for the evaluation which has sufficient nonlinearity, including multiple minimum, to assess the vibration reduction capability of the adaptive controllers. The adaptive control algorithms are based upon a linear transfer matrix assumption and the presence of nonlinearity is shown to have a significant effect on algorithm behavior.

Simulation results are presented which demonstrate the importance of the caution property in the global linear controller. Caution is represented by a time varying rate weighting term in the local linear controller and this is found to improve algorithm convergence. Nonlinearity in some cases is found to cause Kalman filter divergence. Two forms of the Kalman filter covariance equation are investigated. Several deficiences are isolated in the adaptive controllers and recommendations presented for improvement. Areas requiring further research are outlined.

INTRODUCTION

Adaptive control techniques for higher harmonic control (HHC) of helicopter vibration have been used in wind tunnel tests [1,2,3] and simulation models[4,5,6]. A summary of this activity is reported in ref. 3 and ref. 5. The use of adaptive control concepts rather than classical constant gain controllers has emerged because constant gain controllers have resulted in unsatisfactory vibration reduction[1-6]. Nonlinearity has been suspect as one possible explanation for the poor results, however most research has focused on using the linear transfer matrix model in adaptive controller design. The adaptive controllers treat the transfer matrix as an unknown but time varying quantity, and thus the adaptive solution accounts for nonlinearity in an indirect manner. Although nonlinearity is not directly accounted for in the control design, the demonstrated performance of the adaptive control solutions have been successful in many cases [1,2,3,4]. An investigation of nonlinearity on the convergence behavior of adaptive controllers which are based upon the linear transfer matrix is presented.

A nonlinear model assumed to be representative of vibration is selected for the investigation. The model is selected to be complex enough to represent quadratic nonlinearity and yield multiple minimum solutions of the objective function, yet simple enough to provide a clear peiture of algorithm convergence behavior. Simulations and graphical presentation of the vibration model are presented.

Three control concepts are investigated; 1) the local linear adaptive controller reported in ref. 5, and ref. 6, 2) the global linear controller (deterministic) of ref. 1 and ref. 3, and 3) the global linear controller with caution of ref. 1 and ref. 3. The local linear model of ref. 5 and ref. 6 is similar to that in ref. 4 and thus it is expected to represent similar behavior. In addition, the local linear controller includes constant rate weighting as well as time-varying rate weighting. Limited control authority (i.e. $u_{min} \leq u \leq u_{max}$) is employed as well as control rate authority limits. The control algorithms investigated are simulated as close as is practical to the manner in which they would be used in wind tunnel, flight test, or simulation experiments.

Since the algorithms inherently contain a linear Kalman filter, the effect of nonlinearity violates the assumptions used in the Kalman filter derivation. This model mismatch can lead to Kalman filter divergence. The validity of the Kalman filter estimate and covariance is discussed.

The results presented attempt to quantify the importance of nonlinearity on adaptive control algorithm performance. The simulation model used in the investigation, although of limited complexity, is believed to represent the type of nonlinearity encountered in actual helicopter vibration. Thus, the convergence behavior of the adaptive algorithm can be considered as representative of that expected in wind tunnel or flight test application.

SYMBOLS

B	Control matrix used in the global and local linear vibration model in Eq. (2.6) and Eq. (2.20), respectively
$\hat{B}$	estimated control matrix
$C(k)$	cost function from time step k
$E(\ )$	denotes expected value
$E(\cdot\|\cdot)$	denotes conditional expected value
$f(\ )$	general nonlinear vector valued function
H	measurement matrix used in the Kalman filter; for the global model defined in Eq. (2.14), for the local model defined in Eq. (2.27)
i	time step number
J	expected value of the cost function
j	control index number used in Eq. (2.11) and (2.12)
K	Kalman gain matrix defined in Eq. (2.16)
k	time step number
P	Parameter Covariance matrix used in Eq. (2.17)
Q	weighting matrix on the state (vibration amplitude)
q_j	individual elements of the weighting matrix
R	weighting matrix on the controls
R_Δ	rate weighting matrix on control change
u	control vector
u^*	optimal control for the global linear adaptive controller, given by Eq. (2.10)
Δu	control vector change from kth to k+1 step
Δu_{CE}	certainty equivalent control solution for the local linear adaptive controller computed in Eq. (2.26)
u_{min}, u_{max}	minimum and maximum control magnitude limits, respectively
$\Delta u_{min}, \Delta u_{max}$	minimum and maximum control change limits, respectively
V	process noise covariance matrix

W	measurement noise covariance matrix
w	discrete time zero mean white measurement noise
w'	discrete time zero mean white measurement noise on the difference between two successive measurements
x	state vector (vector of vibration sine or cosine amplitude component)
x_o	state vector with zero control
$\tilde{x}$	state vector of vibrations in the nonlinear model
y	measurement vector
Y^{N-1}	information set $Y^{N-1} = \{y^{n-1}, y^{n-2}, \ldots . y^1\}$
α	scalar step-size parameter used in Newton-Raphson algorithm
Θ	parameter vector in the nonlinear model of Eq. (2.1)
$\hat{\Theta}$	estimated parameter vector
$( )^T$	denotes transpose
$( )^{-1}$	denotes matrix inverse

SIMULATION MODEL AND ADAPTIVE CONTROLLERS

This section summarizes the simulation model and the adaptive controllers used in this investigation. These control algorithms are the same as those reported in ref. 3 and ref. 5 and a complete description of the control algorithms are presented in this section for completeness. Three basic controllers are investigated; 1) the global linear controller of ref. 1 and 3, 2) the global linear controller with caution of ref. 1 and ref. 3, and 3) the local linear adaptive controller of ref. 5 and 6.

Simulation Model and Overall Approach

The nonlinear simulation model is selected to contain significant nonlinearity which includes up to second order terms of a Taylor series expansion about zero HHC. The simulation does not represent a physical helicopter model but is chosen based upon the objective to assess the importance of nonlinearity on control algorithm convergence. The nonlinear model parameter values were obtained from ref. 7. The model selected is a subset of a larger model used for the Controllable Twist Rotor (CTR) aeroelastic simulation program (ref. 7). Ref. 7 parameter values were chosen because of their availability and the fact that significant nonlinearity of HHC is present in the model. The signs were changed on the nonlinear terms to yield multiple minimum solutions. It was found that when using the original signs on the nonlinear terms the minimum cost function was nearly the same value as with zero HHC. Therefore, the signs were altered to simulate a more realistic multiple minima vibration problem.

The nonlinear simulation model used is

$$x_1(k+1) = \Theta_1 + \Theta_2\, u_1(k) + \Theta_3\, u_2(k) + \Theta_4\, u_1^2(k) + \Theta_5\, u_2^2(k) + \Theta_6\, u_1(k)\, u_2(k) \qquad (2.1)$$

$$x_2(k+1) = \Theta_7 + \Theta_8\, u_1(k) + \Theta_9\, u_2(k) + \Theta_{10}\, u_1^2(k) + \Theta_{11}\, u_2^2(k) + \Theta_{12}\, u_1(k)\, u_2(k)$$

where the state x_1 and x_2 represent hub shear and blade bending moment amplitude in lbs. and in -lbs., respectively of 4 per rev vibration (for a 4-bladed rotor). The controls u_1 and u_2 represent higher harmonic control amplitude in degrees.

The simulation parameter values are

$$\begin{aligned} \Theta_1 &= 287.3 & \Theta_7 &= 4410. \\ \Theta_2 &= -25.1 & \Theta_8 &= -32.5 \\ \Theta_3 &= +14.4 & \Theta_9 &= -54.0 \\ \Theta_4 &= -6.4 & \Theta_{10} &= -60.6 \\ \Theta_5 &= -19.2 & \Theta_{11} &= -87.3 \\ \Theta_6 &= +6.9 & \Theta_{12} &= +98.6 \end{aligned} \tag{2.2}$$

The measurement model is

$$\begin{aligned} y_1(k) &= x_1(k) + w_1(k) \\ y_2(k) &= x_2(k) + w_2(k) \end{aligned} \tag{2.3}$$

where w_1 and w_2 are zero mean gaussian random white noise sequences with covariance

$$E\{w(k)\ w^T(j)\} = W\delta_{kj} \tag{2.4}$$

where $W_{11} = 28^2$ and $W_{22} = 440^2$. This covariance represents a 10% noise level on the model of Eq. (2.1) with zero HHC.

Examination of the magnitude of the parameter values of Eq. (2.2) reveals significant nonlinearity due to the squared terms and cross-product HHC.

The simulations performed are intended to represent the algorithm convergence about a steady flight condition. The speed of convergence and stability of the algorithm at a steady flight condition will determine to a large degree the algorithm behavior as the helicopter maneuvers or changes flight condition. If convergence is rapid and the algorithm very stable, then the control solution may be more suitable for a varying flight condition. Slow convergence behavior or poor stability of the algorithm indicates that the algorithm may then have difficulty keeping vibrations low during changing flight conditions. Thus, the convergence behavior about a steady nonlinear condition can be used qualitatively to assess vibration reduction capability in maneuvering flight.

The overall approach taken in this investigation, is to use the model defined in Eq. (2.1) through (2.4) as the true model. The adaptive control algorithms are based upon a linear representation to this model. Both a local linearization and global linearization is used.

Global Linear Adaptive Controller

The nonlinear model of Eq. (2.1) is represented as

$$\tilde{x}(k+1) = x_o + f(\Theta, u(k)) \tag{2.5}$$

where x_o is an unknown parameter vector and $f(\Theta, u(k))$ is the general nonlinear function (Eq. (2.1)) of parameter Θ and HHC $u(k)$. The state of the nonlinear model is denoted by $\tilde{x}(k+1)$.

The global linear model representation is

$$x(k+1) = x_o + B\, u(k) \tag{2.6}$$

where B is a matrix of unknown parameters. The model of Eq. (2.6) is intended to represent the global nonlinear model of Eq. (2.5). As such, the parameters in B will not correspond in general to the linear parameters in Eq. (2.1). The unknown elements of x_o and B are denoted as Θ with covariance P.

Measurements are made on the nonlinear simulation model and are given by

$$y(k) = \tilde{x}(k) + w(k) \tag{2.7}$$

where

$$E[w(k)] = 0\ , \quad E[w(k)w^T(j)] = W\delta_{kj} \tag{2.8}$$

The general vibration criterion to be minimized is the expected value of the cost from step 0 to N

$$J(0) = E\{C(0)\} = E\left\{\sum_{k=1}^{N} x^T(k)\ Q\ x(k) + u^T(k-1)\ R\ u(k-1)\right\} \tag{2.9}$$

A one step control solution is obtained by minimizing Eq. (2.9) for N-1 (ref. 3 and ref. 8)

$$u^*(N-1) = -[R + E(B^T\ Q\ B|Y^{N-1})]^{-1}\ E(B^T\ Q\ x_o|Y^{N-1}) \tag{2.10}$$

where the conditional expectation is given by

$$E(B^T\ Q\ B|Y^{N-1}) = \hat{B}^T\ Q\ \hat{B} + \sum_{j=1}^{n} q_j\ \mathrm{cov}(B_{ji}, B_{j\ell}) \tag{2.11}$$

$$E[B^T\ Q\ x_o|Y^{N-1}] = \hat{B}^T\ Q\ \hat{x}_o + \sum_{j=1}^{n} q_j\ \mathrm{cov}(B_{ji}, x_{oj}) \tag{2.12}$$

The parameter estimates $\hat{B}$, $\hat{x}_o$ and the covariances are obtained from a linear Kalman filter where $\hat{B}$ and $\hat{x}_o$ are defined as

$$\hat{x}_o = \begin{bmatrix} \hat{\Theta}_1 \\ \hat{\Theta}_7 \end{bmatrix} \quad , \quad \hat{B} = \begin{bmatrix} \hat{\Theta}_2 & \hat{\Theta}_3 \\ \hat{\Theta}_8 & \hat{\Theta}_9 \end{bmatrix} \tag{2.12a}$$

The global linear model of Eq. (2.6) is modeled as

$$y(k) = H(k)\ \Theta + w(k) \tag{2.13}$$

where

$$H(k) = \begin{bmatrix} 1 & u_1(k) & u_2(k) & 0 & 0 & 0 \\ 0 & 0 & 0 & 1 & u_1(k) & u_2(k) \end{bmatrix} \tag{2.14}$$

The Kalman filter estimate of Θ and covariance is given by (ref. 9)

$$\hat{\Theta}(k+1) = \hat{\Theta}(k) + K(k+1)(y(k+1)) - H^T(k)\ \Theta(k)) \tag{2.15}$$

$$K(k+1) = P(k)\ H^T(k)(W + H(k)\ P(k)\ H^T(k))^{-1} \tag{2.16}$$

$$P(k+1) = P(k) - K(k+1)H(k)\ P(k) + V \tag{2.17}$$

Eqs. (2.15) through (2.17) represent the original Kalman form of the solution for estimation of parameters Θ. An alternate form for the covariance equation is also investigated which retains positive definiteness better than Eq. (2.17). The numerically more accurate alternate form (ref. 10) is

$$P(k+1) = (I - K(k+1)\ H(k))\ P(k)(I - K(k+1)\ H(k))^T + K(k+1)\ W\ K^T(k+1) + V \tag{2.18}$$

A third form of the Kalman filter which replaces the process noise covariance V in Eq. (2.17) is obtained using an exponentially weighted least square formulation (ref. 9). This form is obtained from Eq. (2.16) and (2.17) by multiplying the covariance at step k with the forgetting factor $1/\lambda$, where $\lambda < 1$ (typically chosen to be .99). The exponentially weighted form is obtained by replacing P(k) with $P(k)/\lambda$ and setting $V = 0$. The forgetting factor replaces the process noise covariance and keeps the covariance and Kalman gain from approaching zero as more and more data is processed.

An advantage of the forgetting factor form over Kalman form in Eq. (2.16) and (2.17) is that only a single number (λ) need by selected a priori in using the filter. In the Kalman form the covariance V has n diagonal elements, one for each parameter.

It was found that sometimes loss of positive definiteness occurred with the covariance equation of Eq. (2.17). Because of this the alternate form of the covariance equation (Eq. (2.18)), and the filter with forgetting factor P(k) replaced with P(k)/λ) are used throughout the simulations.

Local Linear Adaptive Controller

The local linear model represents a small perturbation about the current HHC value. Evaluating the measurement y(k+1) at time step k+1 in Eq. (2.7) and subtracting Eq. (2.7) from this results in

$$y(k+1) = y(k) + f(u(k), \Theta) - f(u(k-1), \Theta) + w(k+1) - w(k) \tag{2.19}$$

Approximation of the nonlinear functions in Eq. (2.19) and linearizing the right hand side of Eq. (2.19) results in

$$y(k+1) = y(k) + B(k)\ \Delta u(k) + w'(k+1) \tag{2.20}$$

where at time step k,

$$\Delta u(k) = u(k) - u(k-1) \tag{2.21}$$

$$B(k) = \left.\frac{\partial f}{\partial u}\right|_k = \left.\frac{\partial f}{\partial u}\right|_{k+1} \tag{2.22}$$

$$w'(k+1) = w(k+1) - w(k) \tag{2.23}$$

The local model of Eq. (2.20) has twice the noise covariance of the global model as shown in Eq. (2.23). The noise covariance is

$$E[w'(k)\ w'^{T}(j)] = \begin{cases} 2W\ \delta_{kj} & , \quad k = j \\ -W\ \delta_{kj} & , \quad k = 1,\ j = 2 \text{ and } k = 2,\ j = 1 \\ 0 & , \quad \text{for all other values of k and j} \end{cases} \tag{2.24}$$

As shown in Eq. (2.24) the measurement noise is no longer uncorrelated upon taking the difference between two successive measurements. The Kalman filter formulation which follows assumes the noise is uncorrelated with covariance equal $2W\ \delta_{kj}$ for $k = j$ and zero for all other values of k and j. The effect of this assumption on the accuracy of the Kalman filter estimate is not known, however the correct correlated form can be implemented as in Ref. 10.

The global vibration criterion to be minimized is

$$J(0) = E\{C(0)\} = E\left\{\sum_{k=1}^{N} y^{T}(k)\ Q\ y(k) + u^{T}(k-1)\ R\ u(k-1)\right.$$

$$\left. + \Delta u^{T}(k-1)\ R_{\Delta}\ \Delta u(k-1)\right\} \tag{2.25}$$

The rate weighting term R_Δ is included and penalizes the control for taking too large a step size. It is noted that the rate weighting term is similar to the caution property, however the value of R_Δ must be selected as a design parameter. The caution property in the global model is based upon the covariance matrix P, which is automatically determined in the Kalman filter and is also time varying.

The control required to minimize the objective function of Eq. (2.25) for one time step is

$$\Delta u_{CE}(k) = -(R + R_\Delta + \hat{B}^T Q \hat{B})^{-1}(\hat{B}^T Q y(k) + R u(k)) \tag{2.26}$$

where $\hat{B}$ is obtained from a Kalman filter. A better approach is to estimate $\hat{B}$ and $\hat{y}(k)$ with a modified Kalman filter. However $y(k)$ is used in Eq. (2.26) to be consistent with the formulation used in ref. 5 and ref. 6.

The Kalman filter solution of Eq. (2.15) through Eq. (2.17) is used with the following definitions

$$H = \begin{bmatrix} \Delta u_1(k) & \Delta u_2(k) & 0 & 0 \\ 0 & 0 & \Delta u_1(k) & \Delta u_2(k) \end{bmatrix} \tag{2.27}$$

$$y(k+1) \quad \text{replaced by} \quad y(k+1) - y(k) \tag{2.28}$$

$$W \quad \text{replaced by} \quad 2W \tag{2.29}$$

The local linear adaptive controller consists of Eq. (2.26) and definitions of Eq. (2.27) through (2.29) used in the Kalman Filter. The alternate form of the covariance equation and forgetting factor form is applicable.

GRAPHICAL DESCRIPTION OF THE NONLINEAR VIBRATION SIMULATION

This section presents a graphical description of the nonlinear vibration model defined in Eq. (2.1) and Eq. (2.2). In addition detailed plots are presented of the one step deterministic optimization criterion (i.e. sum of squares of vibration sine and cosine amplitudes). A Newton Raphson off-line type algorithm is used on the objective function to obtain the HHC which minimizes the objective function.

Graphical Description of the Vibration Model

The equations used for the nonlinear vibration model are shown in Eq. (2.1) and Eq. (2.2). The vibration component amplitude term x_1 is shown plotted in figure 1 and x_2 is shown in figure 2. The vertical axis represents the vibration component amplitude and the horizontal axes represents the HHC u_1 and u_2. The control axis is shown for $-10^o \leq u_1 \leq 10^o$ and $-10^o \leq u_2 \leq +10^o$. The nonlinear curvature (quadratic) is clearly shown in figure 1 and figure 2. If nonlinearity was absent the curves would describe the surface of a plane.

The objective function for minimization is selected as shown in Eq. 3.1.

$$J = E\{q_1 x_1^2(1) + q_2 x_2^2(1) + r_1 u_1^2(0) + r_2 u_2^2(0)\} \qquad (3.1)$$

where, $q_1 = 10^{-5}$, $q_2 = 5 \times 10^{-8}$, $r_1 = 10^{-4}$, and $r_2 = 10^{-4}$. The values of q_1 and q_2 were chosen approximately as $1/x_1^2$ and $1/x_2^2$ at zero HHC, respectively. The control weightings r_1 and r_2 were chosen very small and thus their effect is negligible. The criterion for minimization (Eq. (3.1)) is shown plotted in figure 3 through figure 5 with different ranges of u_1 and u_2. Figure 3 shows the cost plotted for $-10 \leq u_1 \leq +10$ and $-10 \leq u_2 \leq +10$. The value of J at $u_1 = u_2 = 0$ is

$$J\Big|_{u_1=u_2=0} = 10^{-5}(287.3)^2 + 5 \times 10^{-8}(4410)^2 = 1.797 \qquad (3.2)$$

A slight "bubble" occurs centered around $u_1=u_2=0$ as seen in the figures. This is more clearly seen in Fig. 4 and Fig. 5. This results in a local maximum and the cost decreases as u_1 and u_2 move away from the [0, 0] coordinate and is more clearly shown in figure 4 and figure 5.

The graphical description of the cost function of figure 3 through figure 5 indicates the presence of multiple minima solutions as well as a local maximum. The range of u_1 and u_2 plotted in these figures does not provide sufficient resolution to pinpoint the local minimum solutions. In figure 5, 4 regions are defined corresponding to the 4 quadrants I, II, III and IV. These are defined as

Region I : $0 \leq u_1 \leq +10, \quad -10 \leq u_2 \leq 0$

Region II : $0 \leq u_1 \leq +10, \quad 0 \leq u_2 \leq +10$

Region III: $-10 \leq u_1 \leq 0, \quad 0 \leq u_2 \leq 10$

Region IV : $-10 \leq u_1 \leq 0, \quad -10 \leq u_2 \leq 0$

Part of Region I ($0 \leq u_1 \leq 10, -1 \leq u_2 \leq 0$) is shown graphically in figure 6 which shows the presence of a valley. Parts of Region I and II combined ($-10 \leq u_1 \leq +10, -1 \leq u_1 \leq 0$) is shown in figure 7 which shows the presence of two valleys. Although the graphical portrayals allows a detailed examination into the shape of the nonlinear surface the precise minimum point cannot be determined. A Newton-type search algorithm is used to locate the local minimum solutions.

Newton's Search For Local Minimum Solutions

A modified Newton-Raphson algorithm was applied to the cost function of Eq. (3.1) with the nonlinear vibration model of Eq. (2.1) and (2.2). The modified Newton method iterates on the cost while updating the HHC u_1 and u_2 at each iteration according to

$$u^{j+1} = u^j + \alpha \left[\frac{\partial^2 J}{\partial u \partial u}\right]^{-1} \frac{\partial J}{\partial u} \qquad (3.3)$$

The gradient $\frac{\partial J}{\partial u}$ and second gradient (Hessian) are computed numerically in the Newton algorithm. The step-size parameter α is chosen to keep the magnitude of the update from iteration to iteration reasonably small.

The Newton-Raphson algorithm was started at three different starting points corresponding to Region I, Region III, and Region IV of figure 5. Three local minimum solutions were found as follows;

Region I : $u^* = [5.37 \quad -.729]^T$, $J^* = .3035$ (83% reduction)

Region III: $u^* = [-6.15 \quad 2.58]^T$, $J^* = .022$ (98.77% reduction)

Region IV : $u^* = [-9.03 \quad -.29]^T$, $J^* = .025$ (98.60% reduction)

The cost J for zero HHC input was computed in Eq. (3.2) ($J = 1.797$ with $u_1 = u_2 = 0$). The percentage reduction is 83%, 98.77%, and 98.60% for Regions I, III, and IV, respectively. Increasing the allowable iterations in the Newton search would permit slightly smaller cost values, however the % reductions obtained can be considered as the approximate local minimum solutions.

The local minimum solutions obtained using the Newton algorithm are used for comparing the minimum values obtained using the adaptive controllers of the next section.

SIMULATION RESULTS OF THE GLOBAL LINEAR ADAPTIVE CONTROLLER

This section presents the results of the global linear adaptive controller presented in Section II. Two versions of the controller are simulated; 1) the deterministic version based on the certainty equivalence (CE) property of stochastic control and the, 2) the cautious controller. The CE control assumes the covariance P of the parameter estimate is zero. First, results from a linear simulation model is discussed and then detailed results using the nonlinear model of Eq. (2.1) are presented.

Controller Initialization and Authority Limits

The use of the global adaptive controller requires initialization of the parameters and covariance. Although there are many ways to obtain initialization the initial parameter estimates were generated from a random number generator with normal distribution $N(\Theta_i(0), P_{ii}(0))$, $i=1,2,\ldots,M$, where the covariance was set to $\Theta_i^2(0)$. An equally valid initialization would be to guess arbitrarily non-zero values for the parameters and select the covariance to be reasonably large.

During simulation with the nonlinear model it was found that the CE global adaptive controller and local adaptive controller would often exceed the practical range of control. Therefore, a software control authority limiter was used on the controllers and also rate limiting was used on the local controller.

The need for control limits arises because of either; 1) poor parameter estimates or 2) nonlinearity in the vibration model which result in very large magnitude control. Limiters were also used in reference 1, 3 and 4.

The form of the control authority magnitude limits used are

$$\begin{aligned} u_{1MIN} \leq u_1 \leq u_{1MAX} \\ u_{2MIN} \leq u_2 \leq u_{2MAX} \end{aligned} \tag{4.1}$$

and the control authority rate limits are

$$\begin{aligned} \Delta u_{1MIN} \leq \Delta u_1 \leq \Delta u_{1MAX} \\ \Delta u_{2MIN} \leq \Delta u_2 \leq \Delta u_{2MAX} \end{aligned} \tag{4.2}$$

The global linear adaptive controller with caution never required rate limiting, since the caution property is in fact a time varying rate limiter. The local model was also used with a rate limit weighting term R_Δ in the cost function (Eq. 2.25). Both constant and time varying R_Δ are used. For the simulation runs, the specific control authority magnitude limits and rate limits will be clearly indicated. The selection of appropriate magnitude and rate limits is very important to convergence behavior for the global linear adaptive CE controller and the local linear controller and is likely dependent on this nonlinear

plant model. Also for the nonlinear model simulation runs the selection of suitable control magnitude limits dictates which local minimum region (see (fig. 5) the controller will converge to.

Linear Simulation Runs

The focus of this investigation is on the effect of nonlinearity in the vibration model. Linear simulation runs were investigated in detail in reference 6 for a different simulation model. Detailed linear simulation runs were done in reference 1 before testing on the wind tunnel. It was stated in ref. 1 that all controllers tested performed satisfactorily on the linear simulation and the performance was significantly different in the wind tunnel. The linear simulation results obtained in reference 1 are similar to that obtained here.

The linear simulation model used is that shown in Eq. (2.1) with all nonlinear terms set to zero. The vibration reduction is shown in figure 8 which shows the average cost of 100 monte carlo computer runs for different initial conditions and noise sequences. No magnitude or rate limiting is used. The CE control takes a very large control step in the beginning due to parameter uncertainty and this results in large vibrations and cost.

The cautious control accounts for parameter uncertainty and thus the cost goes down at every step. Figure 8 also shows rapid convergence for both CE and cautious control. The large initial step in the CE control causes rapid parameter identification and thus the cost rapidly converges. The CE control in the first two time steps could be improved with a magnitude and rate limiter to avoid large control inputs, but this was not done.

The main finding for the linear simulation is that both the CE control and cautious control convergence is 4 to 8 time steps. The CE control requires magnitude and possibly rate limiting.

The next section demonstrates the effect of nonlinearity on algorithm convergence.

Nonlinear Simulation Results, CE Controller

The nonlinear simulation of Eq. (2.1) is used with the global linear CE control of Eq. (2.10) with covariance P = 0. The forgetting factor λ is set to 1 (i.e. no forgetting factor) and the magnitude control limits used are

$$\begin{aligned} -10 \leq u_1 \leq +10 \\ -10 \leq u_2 \leq +10 \end{aligned} \qquad (4.3)$$

The computed control, state, and cost at k = 1 using the initial parameter estimates and covariance as discussed previously are

$$u_{CE}(1) = \begin{bmatrix} -10. \\ -10. \end{bmatrix}, \quad x(1) = \begin{bmatrix} -1475.0 \\ 365.0 \end{bmatrix}, \quad J(1) = 21.7 \qquad (4.4)$$

The control immediately reached the magnitude limits -10 and increased the cost from 2.8 to 21.7. This should be compared to the 1st time step for the linear

model in figure 8 which increases the average cost (shown is the average of 100 runs) to 8.8. The nonlinearity causes a dramatic increase in cost even with the control magnitude limiter of ± 10. Figure 9 shows the convergence of the cost and controls u_1 and u_2 for 100 time steps. The initial points for the first 6 steps are off the scale in figure 9d which is an expanded scale of figure 9a. Convergence at time step 100 is

$$u_{CE}(100) = \begin{bmatrix} -10 \\ -1.1 \end{bmatrix}, \quad x(100) = \begin{bmatrix} -64. \\ -278. \end{bmatrix}, \quad J(100) = .045 \qquad (4.5)$$

Convergence occurs in Region IV of the nonlinear cost surface (see figure 5). Convergence is good only after the excessive control magnitudes die out.

The large magnitude control changes indicate the need for rate limiting. Rate limiting was used in the wind tunnel tests of reference 1 and reference 3 on this controller. The cautious control of the next section inherently includes a rate limiting effect and its operation is significantly improved over the CE control.

Nonlinear Simulation Results, Cautious Controller

The global linear cautious controller of Eq. (2.10) is used with the nonlinear simulation model of Eq. (2.1). The cautious controller was used with $\lambda = 1$ (no forgetting factor) and $\lambda = .99$ (with forgetting factor). As discussed previously the forgetting factor is used in place of the process noise covariance on the parameters to account for random variation of the parameters. In addition, three different values are used for the initial estimate of the covariance, P(0), P(0)x10, and P(0)x100.

The convergence results are summarized in Table 1 for the cautious controller. Convergence is restricted to Region III and Region IV (see figure 5) using the control magnitude limits

$$\begin{aligned} -10 \le u_1 \le -8 \\ -3 \le u_2 \le 5 \end{aligned} \qquad (4.6)$$

The control magnitude limits (Eq. (4.6)) constrain the control to the local minimum solution of Region III and Region IV. Newton's off-line method which was discussed in section III converged to $u^* = [-9.03 \quad -.29]^T$ with $J^* = .025$. This point is the approximate minimum solution. The cautious controller for run 3a, 2b and 3b of Table 1 converged to a slightly lower minimum point.

The results of Table 1 show that increasing the initial covariance clearly improves convergence. Since the Kalman filter is based upon a linear model, increasing the initial covariance causes smaller control changes initially where the surface is very nonlinear. The linear transfer matrix model used in the Kalman filter design is a very poor representation where the surface is nonlinear. Thus, increasing the initial covariance is required to offset the nonlinearity. Note that this is not required for the linear simulation.

Figure 10 (Run 1a of Table 1) shows results for P(0)x1, figure 11 (Run 2b) for P(0)x10 and, figure 12 (Run 3a) for P(0)x100. Convergence results improve as P(0) is increased. It is expected that increasing P(0) further would degrade performance due to too much caution resulting in slow convergence.

Table 1 also shows results with and without the forgetting factor. The results are similar either with forgetting factor or without except for P(0)x10 (Run 2b of Table 1). The forgetting factor prohibits the covariance from decreasing as fast as without the forgetting factor, thus the caution effect is larger. More caution yields better convergence.

In summary, the global linear adaptive controller (with caution) results in excellent convergence as shown in figure 12. However, to achieve this excellent convergence the initial covariance must be selected larger for the nonlinear simulation model than for a linear simulation model. Multiplying the covariance times 100 was required to offset nonlinearities.

SIMULATION RESULTS OF THE LOCAL LINEAR ADAPTIVE CONTROLLER

This section presents the simulation results of the local linear adaptive controller presented in section II. The local adaptive controller is simulated on the nonlinear model and three different control rate limiting terms are investigated; 1) R_Δ = constant, 2) $R_\Delta = K/i$, and 3) $R_\Delta = K/i^2$. In all simulation runs both a magnitude limiter (Eq. (4.1)) and rate limiter (Eq. (4.2)) are used. The controller initialization is performed in a similar manner to the global adaptive controller as discussed in section IV.

Local Linear Adaptive Controller With Rate Weighting

The local linear adaptive controller of Eq. (2.26) through Eq. (2.29) was simulated on the nonlinear model of Eq. (2.1). The magnitude and rate limiter used is

$$\begin{aligned} -10 \le u_1 \le -8 \\ -3 \le u_2 \le +5 \end{aligned} \tag{5.1}$$

and

$$\begin{aligned} -.1 \le \Delta u_1 \le .1 \\ -.1 \le \Delta u_2 \le .1 \end{aligned} \tag{5.2}$$

The magnitude limiter constrains the control to Region III and Region IV of figure 5.

Effect of constant rate weighting on convergence, $R_\Delta = K$. The rate weighting term of the performance criterion of Eq. (2.23) is investigated for $R_\Delta = 0$, $R_\Delta = 1$, and $R_\Delta = 10$. This was done both without the forgetting factor ($\lambda = 1$) and with the forgetting factor ($\lambda = .99$). The results are summarized in Table 2. As indicated in Table 2 convergence is fast for $R_\Delta = 0$, very slow for $R_\Delta = 1$, and very very slow for $R_\Delta = 10$. The stability of the convergence behavior is noted by how oscillatory the solution is. Stability is poorest for $R_\Delta = 0$ and improves for increasing R_Δ. The behavior is similar both with and without forgetting factor.

Figure 13a shows a plot of the cost function of Eq. (2.25) where Q and R are the same as for the global model and $R_\Delta = 0$. Convergence is rapid and occurs for N = 20 time steps and then becomes oscillatory (less stable). Figure 13b and 13c show the corresponding control time histories. Figure 14 shows the cost and controls for $R_\Delta = 1$. Convergence is very slow, however the solution has improved stability. The convergence for $R_\Delta = 0$ is fast (although considerably slower than the global adaptive controller) but very oscillatory. Increasing R_Δ to 1 slows convergence too much to yield acceptable results. A better compromise would be to use a time varying rate weighting.

Effect of time varying rate weighting on convergence, $R_\Delta = K/i$. Table 3 is a repeat of results as in Table 2, with $R_\Delta = 1/i$, $10/i$, and $100/i$. As indicated in the table convergence is either too oscillatory or too slow. For the slow converging runs the control remained in Region IV and the control did not change significantly from its value at the first time step. The rapid convergence runs (Run 1a and 1b of Table 3) went to Region IV and the control u_2 changed sign to positive. Convergence is still unacceptable. A more rapid decrease in R_Δ is investigated next.

Effect of time varying rate weighting on convergence, $R_\Delta = K/i^2$. Table 4 presents convergence results for $R_\Delta = 1/i^2$, $10/i^2$, and $100/i^2$. In all cases convergence occurs in Region III with cost less than that for K or K/i. Convergence is slow for $R_\Delta = 100/i^2$ but faster than for either 100/i or 100. Stability is improved for $R_\Delta = 100/i^2$. Oscillations are slight for $R_\Delta = 10/i^2$ and has slow convergence but faster than $R_\Delta = 10/i$ or $R_\Delta = 10$. Convergence is fast for $R_\Delta = 1/i^2$ but oscillations are large.

Figure 15 shows convergence for $R_\Delta = 1/i^2$, figure 16 for $R_\Delta = 10/i^2$, and figure 17 for $R_\Delta = 100/i^2$. Figure 16 for $R_\Delta = 10/i^2$ shows perhaps the best compromise between stability and fast convergence. However convergence is not nearly as good as the global adaptive controller (see fig. 12) which has very fast convergence (less than 8 time steps) and is also very stable (i.e. there are no oscillations after convergence occurs).

The overall effect of the time varying rate weighting term K/i^2 is to improve the stability (less oscillations) of the control solution. Time varying weighting offers improved flexibility over constant rate weighting in the local adaptive control solution.

Effect of the control rate authority limits on convergence. - As previously indicated the control rate authority limits ($-.1 < \Delta u < .1$) have a significant effect on convergence and algorithm stability. These limits are relaxed to quantify this effect. Figure 18 shows the local linear adaptive controller with $R_\Delta = 0$ and $-.2 \leq \Delta u \leq +.2$. Speed of convergence is increased and convergence occurs in 10 time steps. However the oscillations are more pronounced than for $-.1 \leq \Delta u \leq .1$ (see Fig. 13). Figure 19 shows the rate limits increased to $-.5 \leq \Delta u \leq +.5$. Initially, very wild oscillations occur and persist. Thus, the rate limit authority limits must be kept at $-.1 \leq \Delta u \leq .1$ to retain algorithm stability.

Figure 20 shows the combination of rate authority limits $-.2 \leq \Delta u \leq +.2$ and rate weighting $R_\Delta = .1$. Convergence is slow (20 time steps are required) and divergence occurs. This is compared with figure 14 where $R_\Delta = 1$ and $-.1 \leq \Delta u \leq +.1$. Reducing R_Δ from 1 where convergence is very slow to .1 improves convergence rate but divergence occurs. Repeating this simulation run with $R_\Delta = .1$ and $-.5 \leq \Delta u \leq 5$ resulted in nearly identical convergence as shown in Figure 20.

The results for the local linear adaptive controller show either slow convergence or loss of stability relative to the global linear adaptive controller for the present nonlinear simulation. During the simulation runs a compromise set of values for R_Δ and $\Delta u_{MIN} \leq \Delta u \leq \Delta u_{MAX}$ could not be found which gave results as good as the global linear adaptive controller with caution shown in figure 12.

Kalman Filter Divergence

Kalman filter divergence is a concern in any on-line application which includes a Kalman filter. There are three primary causes of Kalman filter divergence;

1) loss of numerical accuracy due to an accumulation of numerical errors in the recursive covariance equation,

2) model mismatch, and

3) truncation of word length (for example when going from 32 bit to 16 bit word length computer)

The 1st error source (loss of numerical accuracy) is often a result of a poorly conditioned covariance matrix (i.e. the eigenvalue spread is large). Also the recursive nature of the solution causes an accumulation of errors. These errors originate in the matrix multiplication and division required in the covariance equation. Another problem can occur whenever the covariance change from the kth to k+1st step is small. The difference in small numbers causes an accumulation of errors and results in loss of positive definiteness. The alternate form of the covariance equation (Eq. (2.18)) is numerically more accurate for this latter problem.

The 2nd error source (model mismatch) occurs whenever the actual model is different than the model assumed in the Kalman filter. Nonlinearity will cause a model mismatch in the Kalman filter since the Kalman filter is designed based upon a linear representation. An example of divergence due to model mismatch is shown in figure 21. The cost and control time histories are shown for the local linear adaptive controller. The rate weighting is $R_\Delta = 100/i^2$ and the control is constrained in magnitude by $\pm$ 10

$$\begin{aligned} -10 \leq u_1 \leq 10 \\ -10 \leq u_2 \leq 10 \end{aligned} \tag{5.3}$$

The control solution goes into region II (as shown in Fig. 21b and 21c) which is very nonlinear and the model mismatch occurs prior to time step 60 results in divergence after time step 60. Increasing the forgetting factor ($1/\lambda$) or increasing the parameter process noise covariance sometimes will prevent divergence.

Model mismatch divergence can also occur if the parameters are time varying and the time variation is so rapid that the Kalman filter cannot track the parameters. Also for slowly time varying parameters (or constant parameters), if the parameter process noise covariance is too small (or zero) the Kalman gain will be too small to permit proper tracking of the parameters. Kalman filter divergence will result. In reference 6 a linear simulation was done with slowly time varying parameters and Kalman filter divergence is shown (see fig. 12 and fig. 16 of reference 6). The divergence in this reference occurred near the middle and end of the run over 120 time steps. Before complete divergence occurred the controllers recovered. Increasing the process noise covariance or using the alternate covariance Eq. (2.18) could possibly eliminate the divergence altogether.

The 3rd source of error (truncation of word length) occurs because of the recursive nature of the covariance equation. Multiplication and division of matrices cause an accumulation of errors and divergence results. This problem requires special treatment which will not be discussed here. However, when using a 16 bit fixed word length computer Kalman filter divergence is possibly a problem and may require a modification to Eq. (2.15) through Eq. (2.17). All simulation runs done in this report used a 32 bit word length (single precision on an IBM computer).

CONCLUSIONS

A nonlinear simulation was used to analytically investigate nonlinear model effects on linear adaptive control algorithm convergence and stability characteristics. For the simulation used, nonlinearity was found to have a significant effect on HHC algorithm convergence behavior. Linear simulation results showed that convergence to minimum vibrations always occurs in less than 8 time steps (equivalent to 8 rotor revolutions) with either the global linear CE controller (without caution) or global linear cautious controller. The CE controller takes an initial large jump due to lack of caution and then converges rapidly. This initial control input could be overcome by magnitude or rate limiting.

The nonlinear simulation results significantly effect HHC convergence. In addition to multiple minima solutions, the algorithms are generally slower in convergence, less stable, and can result in Kalman filter divergence due to model mismatch. By artifically increasing the initial covariance on the parameter estimates (P(0)x100), the global adaptive cautious controller was found to exhibit excellent convergence in less than 8 time steps. Increasing the covariance has the effect of off-setting nonlinearity by introducing more caution than is required for a linear model. When the initial covariance is too low the convergence behavior is similar to the global linear adaptive controller without caution where the control exhibits a limit cycle between the control limit stops.

The local linear adaptive controller with rate weighting converges very slowly. Without rate weighting ($R_\Delta = 0$), convergence occurs in 20 time steps, however with persistent oscillations. Adding constant rate weighting increases stability (less oscillations), but convergence is very slow (typically 100 time steps or greater). A time varying rate weighting of $R_\Delta = 10/i^2$ improves stability and convergence, yet still requires between 20 and 100 time steps for convergence.

Based upon the simulations performed, the cautious global linear adaptive controller has good convergence and stability and is the superior controller for HHC of vibration. Although the local adaptive controller does converge its susceptability to measurement noise, slow convergence, and tendency to oscillate make this controller less desirable for HHC of vibration in the present study.

Control algorithm speed of convergence and stability determine to an extent the ability to adapt to changing flight conditions. The global cautious controller may be able to track rapidly varying flight conditions. Previous wind tunnel tests in reference 1 and reference 3 have established this tracking capability for the case of increasing airspeed. The local linear adaptive controller may have difficulty tracking rapidly varying flight conditions due to its slower convergence.

The results of this research have isolated several deficiences in the use of higher harmonic control of vibration; 1) Kalman filter divergence, 2) inability to reduce vibrations due to multiple minima solutions, and 3) unpredicted erradic convergence behavior due to nonlinearity. It is recommended that further investigation be undertaken to solve these potential problem areas of HHC.

In addition, research should be further advanced to prohibit Kalman filter divergence. Numerical accuracy, model mismatch, and word length truncation error should be investigated. Finally, there is a need to further reduce the computational burden due to the requirement for on-line Kalman filter calculation and matrix inversion. Algorithms which simplify the computational solution should be investigated.

REFERENCES

1. Hammond C.E., "Wind Tunnel Results Showing Rotor Vibratory Loads Reduction Using Higher Harmonic Blade Pitch," 36th Annual Forum of the AHS, May 1980.

2. Shaw, J., and Albion, N., "Active Control of the Helicopter Rotor for Vibration Reduction," Annual Forum of the American Helicopter Society, Washington, D.C., May 1980.

3. Molusis, J.A., Hammond, C.E., and Cline, J.H., "A Unified Approach to the Optimal Design of Adaptive and Gain Scheduled Controllers to Achieve Minimum Helicopter Rotor Vibration, 37th Annual Forum of the AHS, May 1981.

4. Taylor, R.B., Zwicke, P.E., Gold, P., and Miao, W., "Analytical Design and Evaluation of an Active Control System for Helicopter Vibration Reduction and Gust Response Alleviation," NASA CR 152377, July 1980.

5. Johnson, W., Self-Tuning Regulators for Multicyclic Control of Helicopter Vibration, NASA Technical Paper 1996, March, 1982.

6. Chopra, I. and McCloud, J.L., Considerations of Open-Loop, Closed-Loop, and Adaptive Multicyclic Control Systems, Preprint No. 13, Presented at the American Helicopter Society Northeast Region Specialists' Meeting on Helicopter Vibration, Hartford, Conn., Nov. 1981.

7. Weisbrich, R., Perley, R. and Howes, H., "Design Study of a Feedback Control System for the Multicyclic Flap System Rotor (MFS), NASA CR-151060, Jan. 1977.

8. Bar-Shalom, Y., Mookerjee, P., and Molusis, J.A., A Linear Feedback Controller for a Class of Stochastic Systems, Proceedings of National CNRS College, Oquium "Développement et Utilisation d'Qutils et Modèles Mathématiques en Qutomatique, Analyse de Systèms et Traitement du Signa, Sept. 1982, Belle-Ile, France.

9. Goodwin, G. and Payne, R., Dynamic System Identification: Experiment Design and Data Analysis, Mathematics in Science and Engineering, Vol. 136, Academic Press, 1977.

10. Bryson, A.E. and Ho, Y.C., Applied Optimal Control, Blaisdell Publishing Co., 1969.

Table 1. - Summary of Convergence Results for the Global Linear Adaptive Controller (with caution) using The Nonlinear Simulation. (Refer to figure 5 which shows regions of local minimum solutions).

Run No.	Initial Parameter Covariance	Time Step 1 u(1)	Time Step 1 x(1)	Time Step 1 J(1)	Time Step 100 u(100)	Time Step 100 x(100)	Time Step 100 J(100)	% cost* reduction	Comments	Plot Figure No.
No forgetting factor (λ=1)										
1a.	P(0)	$\begin{bmatrix}-8.\\-3.\end{bmatrix}$	$\begin{bmatrix}28.1\\2534.\end{bmatrix}$	.32	$\begin{bmatrix}-8.\\-2.39\end{bmatrix}$	$\begin{bmatrix}66.33\\2307.\end{bmatrix}$	.31	3.1%	· Poor Convergence · Region IV	---
2a.	P(0)*10	$\begin{bmatrix}-8\\-.745\end{bmatrix}$	$\begin{bmatrix}98.\\1371.\end{bmatrix}$	.19	$\begin{bmatrix}-8.\\-2.08\end{bmatrix}$	$\begin{bmatrix}80.21\\2167.\end{bmatrix}$	.29	Cost increase	· Incorrect Convergence · Region IV	---
3a.	P(0)*100	$\begin{bmatrix}-8\\-.11\end{bmatrix}$	$\begin{bmatrix}82\\884.\end{bmatrix}$	.107	$\begin{bmatrix}-8.0\\1.037\end{bmatrix}$	$\begin{bmatrix}15.53\\-176.3\end{bmatrix}$	.0039	96.3%	· Excellent Convergence · Region III	Fig. 12
With forgetting factor (λ=.99)										
1b.	P(0)	.....(same as 1a).....			$\begin{bmatrix}-8.0\\-2.85\end{bmatrix}$	$\begin{bmatrix}38.3\\2486.\end{bmatrix}$	.32	0%	· Poor Convergence · Region IV	Fig. 10
2b.	P(0)*10	.....(same as 2a).....			$\begin{bmatrix}-8\ 0\\.9611\end{bmatrix}$	$\begin{bmatrix}21.5\\-99.0\end{bmatrix}$	.0051	97.3%	· Erradic jumps in control and cost · Region III	Fig. 11
3b.	P(0)*100	.....(same as 3a).....			$\begin{bmatrix}-8.0\\.98\end{bmatrix}$	$\begin{bmatrix}19.9\\-120.0\end{bmatrix}$	.0046	95.7%	· Excellent convergence · Region III	---

*% cost Reduction improvement over cost at time step 1

Table 2. - Effect of Constant Rate Weighting on Convergence for the Local Linear Adaptive Controller using The Nonlinear Simulation. (Rate limiter on, Magnitude limiter on)

Run No.	Rate Weighting	Time Step 1 u(1)	Time Step 1 x(1)	Time Step 1 J(1)	Time Step 100 u(100)	Time Step 100 x(100)	Time Step 100 J(100)	% Cost* Reduction	Comments	Plot Figure No.
No forgetting factor (λ=1)										
1a	R_Δ=0	$\begin{bmatrix}-8.0\\-0.9\end{bmatrix}$	$\begin{bmatrix}99.6\\1479.\end{bmatrix}$	.208	$\begin{bmatrix}-8.6\\.83\end{bmatrix}$	$\begin{bmatrix}-21.3\\-609.5\end{bmatrix}$	.023	88.9%	• Fast Convergence • Oscillatory • Converged to Region III	Fig. 13
2a	R_Δ=1	$\begin{bmatrix}-8.0\\-.99\end{bmatrix}$	$\begin{bmatrix}100.\\1541.\end{bmatrix}$	.218	$\begin{bmatrix}-8.0\\-.723\end{bmatrix}$	$\begin{bmatrix}97.9\\1355.7\end{bmatrix}$	.187	16.5%	• Very Slow Convergence • No Oscillation • Converged To Region IV	Fig. 14
3a	R_Δ=10	.....(same as 2a).....			$\begin{bmatrix}-8.0\\-.965\end{bmatrix}$	$\begin{bmatrix}99.99\\1523\end{bmatrix}$	.216	0.9%	• Very, Very Slow Convergence • No Oscillation • Converged to Region IV	---
With forgetting factor (λ=.99)										
1b	R_Δ=0	.....(same as 1a).....			$\begin{bmatrix}-8.6\\.79\end{bmatrix}$	$\begin{bmatrix}-17.99\\-563.\end{bmatrix}$	.0101	90.8%	• Fast Convergence • Oscillatory • Converged to Region III	---
2b	R_Δ=1	.....(same as 2a).....			$\begin{bmatrix}-8.0\\-.73\end{bmatrix}$	$\begin{bmatrix}98.\\1360.\end{bmatrix}$	.188	13.7%	• (same as 2a)	---
3b	R_Δ=10	.....(same as 2a).....			$\begin{bmatrix}-8.0\\-.96\end{bmatrix}$	$\begin{bmatrix}99.9\\1523.\end{bmatrix}$	.216	.9%	• (same as 3a)	---

*% cost reduction improvement over cost at time step 1

Table 3. - Effect of Variable Rate Weighting (K/i) on Convergence for the Local Linear Adaptive Controller (Rate and Magnitude Limiter on)

Run No.	Rate Weighting	Time Step 1 u(1)	Time Step 1 x(1)	J(1)	k	Time Step k(1) u(k)	Time Step k(1) x(k)	J(k)	% Cost* Reduction	Comments	Plot Figure No.
No forgetting factor (λ=1)											
1c	R_Δ=1/i	$\begin{bmatrix}-8.0\\-.99\end{bmatrix}$	$\begin{bmatrix}100.\\1541.\end{bmatrix}$	.218	87	$\begin{bmatrix}-8.0\\1.067\end{bmatrix}$	$\begin{bmatrix}13.1\\-207.\end{bmatrix}$	.0038	98.2%	[· medium convergence · oscillatory]	---
2c	R_Δ=10/i				100	$\begin{bmatrix}-8.0\\-.231\end{bmatrix}$	$\begin{bmatrix}86.9\\982.\end{bmatrix}$	.123	43.5%	[· slow convergence · slight oscillation]	---
3c	R_Δ=100/i				100	$\begin{bmatrix}-8.0\\-.84\end{bmatrix}$	$\begin{bmatrix}99.2\\1438.\end{bmatrix}$	.201	7.8%	[· very slow convergence · slight oscillation]	---
With forgetting factor (λ=.99)											
1d	R_Δ=1/i				100	$\begin{bmatrix}-8.0\\1.1\end{bmatrix}$	$\begin{bmatrix}10.1\\-244.\end{bmatrix}$	.004	98.1%	[· medium convergence]	---
2d	R_Δ=10/i				85	$\begin{bmatrix}-8.0\\.415\end{bmatrix}$	$\begin{bmatrix}92.1\\1126.\end{bmatrix}$	.148	32.2%	[· slow convergence]	---
3d	R_Δ=100/i				100	$\begin{bmatrix}-8.0\\-.845\end{bmatrix}$	$\begin{bmatrix}99.2\\1441.\end{bmatrix}$	.202	7.3%	[· very slow convergence]	---

(1) Time step when convergence occurs to minimum

* % cost reduction improvement over cost at time step 1

Table 4. - Effect of Variable Rate Weighting (K/i^2) on Convergence for the Local Linear Adaptive Controller (Rate and Magnitude Limiter on)

Run No.	Rate Weighting	Time Step 1 u(1)	Time Step 1 x(1)	J(1)	k	Time Step k u(k)	Time Step k x(k)	J(k)	% Cost Reduction	Comments	Plot Figure No.
No forgetting factor (λ=1)											
1e	$R_\Delta=1/i^2$	$\begin{bmatrix}-8.0\\-.99\end{bmatrix}$	$\begin{bmatrix}100.\\1541.\end{bmatrix}$	.218	98	$\begin{bmatrix}-8.2\\.88\end{bmatrix}$	$\begin{bmatrix}10.36\\-230.7\end{bmatrix}$	.0037	98.3%	[· fast convergence · oscillatory]	Fig. 15
2e	$R_\Delta=10/i^2$	.....(same as 1e).....			81	$\begin{bmatrix}-8.1\\.92\end{bmatrix}$	$\begin{bmatrix}15.98\\-165.0\end{bmatrix}$	.0039	98.2%	[· medium convergence · slightly oscillatory]	Fig. 16
3e	$R_\Delta=100/i^2$	.....(same as 1e).....			98	$\begin{bmatrix}-8.2\\.89\end{bmatrix}$	$\begin{bmatrix}9.86\\-237.2\end{bmatrix}$	.0037	98.3%	[· slow convergence · no oscillations]	Fig. 17
With forgetting factor (λ=.99)											
1f	$R_\Delta=1/i^2$	.....(same as 1e).....			91	$\begin{bmatrix}-8.1\\1.037\end{bmatrix}$	$\begin{bmatrix}15.5\\-176.\end{bmatrix}$	.0039	98.2%	...same as 1e...	—
2f	$R_\Delta=10/i^2$	.....(same as 1e).....			89	$\begin{bmatrix}-8.0\\1.09\end{bmatrix}$	$\begin{bmatrix}11.1\\-231.\end{bmatrix}$	.0039	98.2%	...same as 2e...	—
3f	$R_\Delta=100/i^2$	.....(same as 1e).....			98	$\begin{bmatrix}-8.23\\.73\end{bmatrix}$	$\begin{bmatrix}18.8\\-109.\end{bmatrix}$	.0041	97.2%	...same as 3e...	—

(1) Time step when convergence occurs. To minimum

a % Reduction in cost improvement over time step 1.

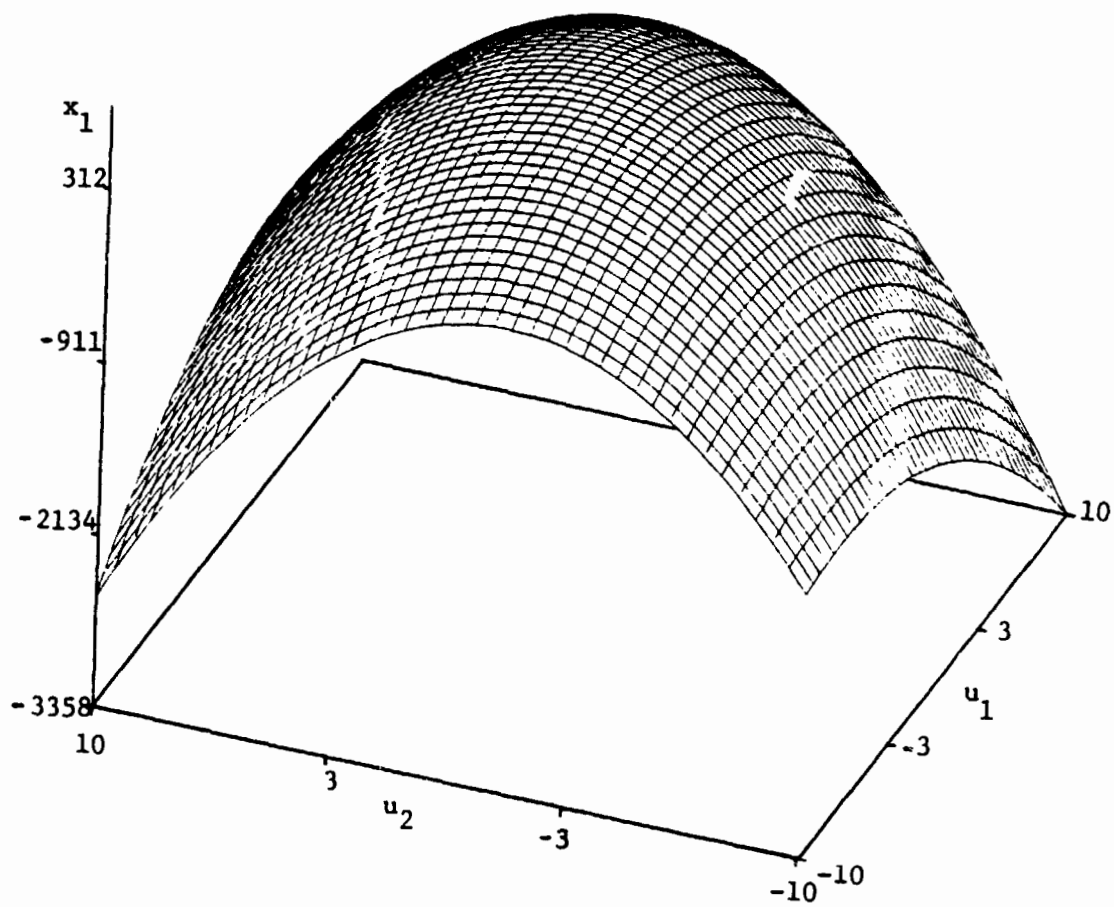

Figure 1. - Vibration State x_1 as a Nonlinear Function of HHC u_1 and u_2.

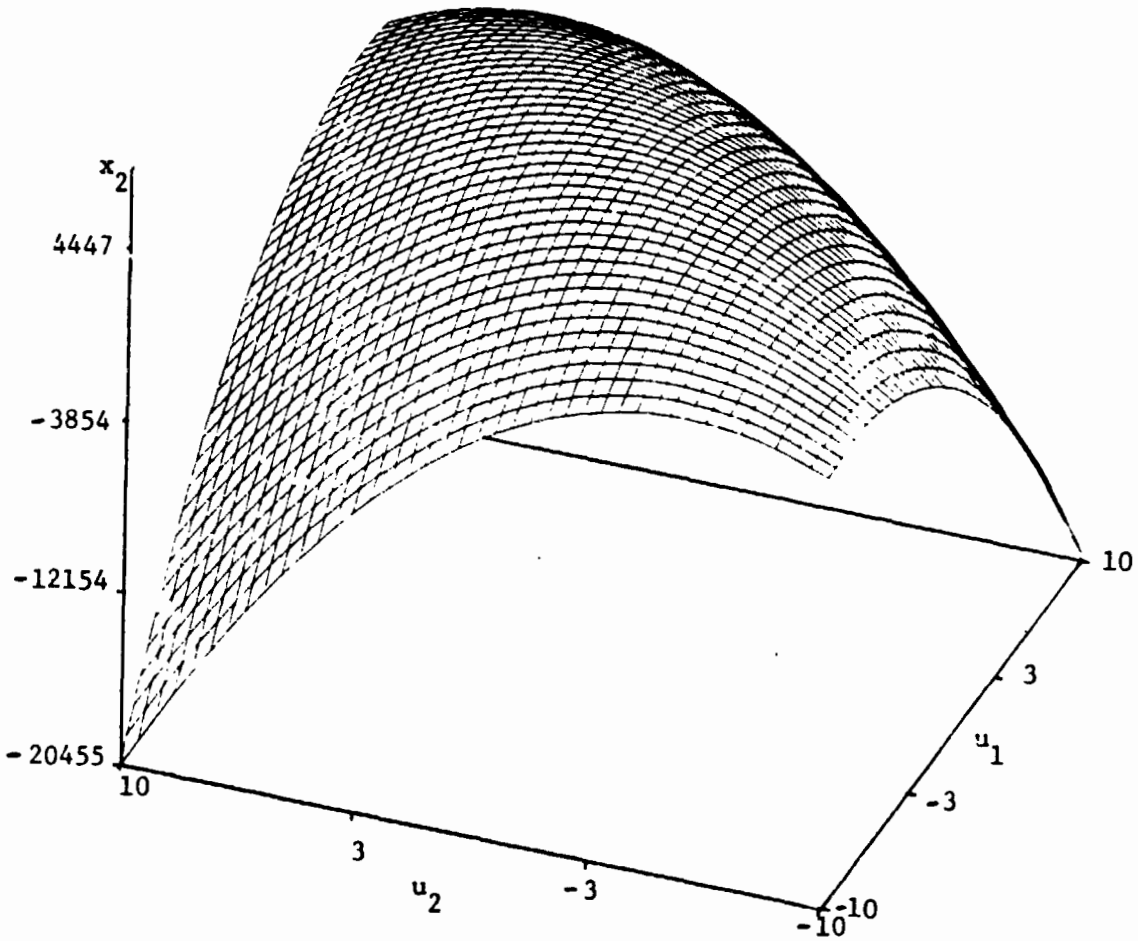

Figure 2. - Vibration State x_2 as a Nonlinear Function of HHC u_1 and u_2.

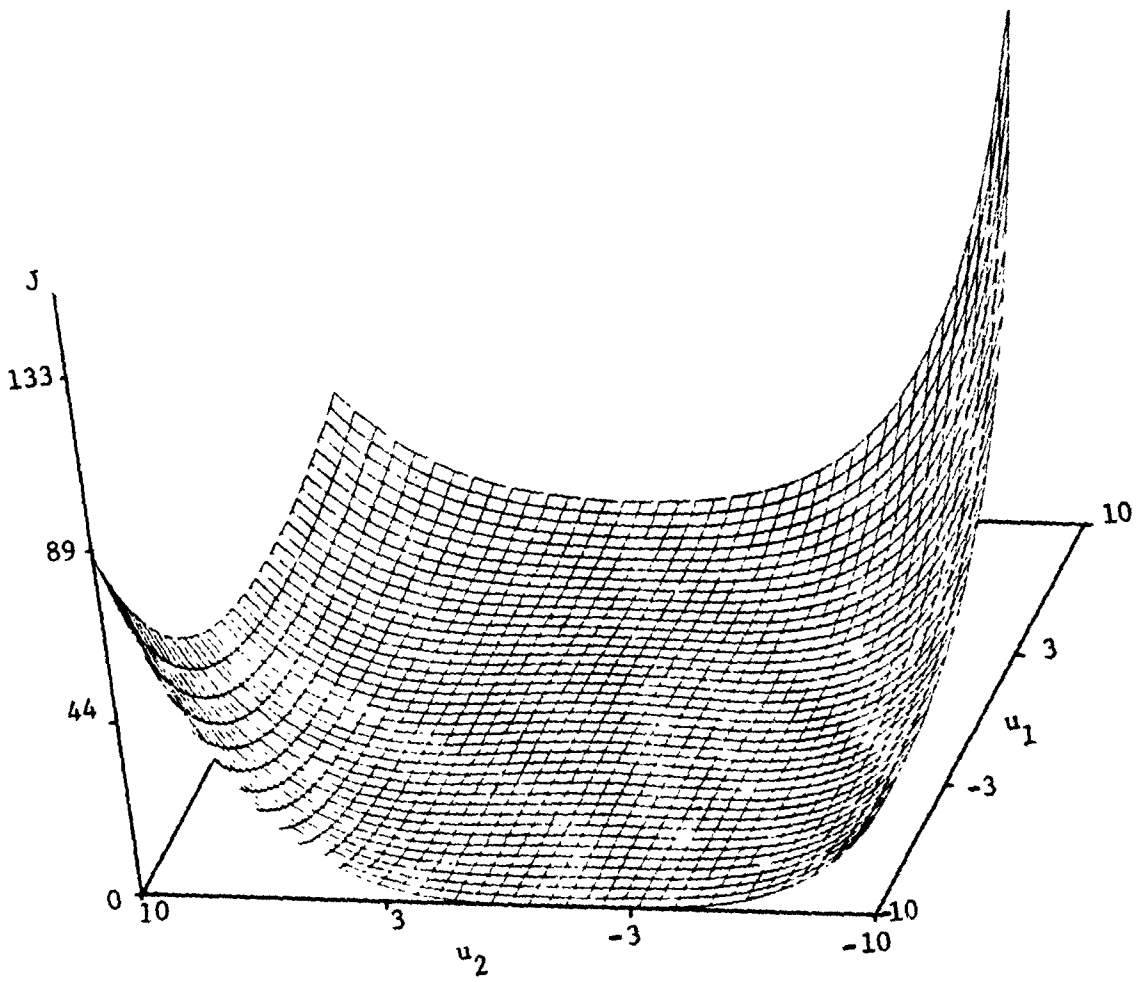

Figure 3. - Quadratic Cost Function as a Nonlinear Function of HHC u_1 and u_2 ($-10 \leq u_1 \leq +10$, $-10 \leq u_2 \leq +10$).

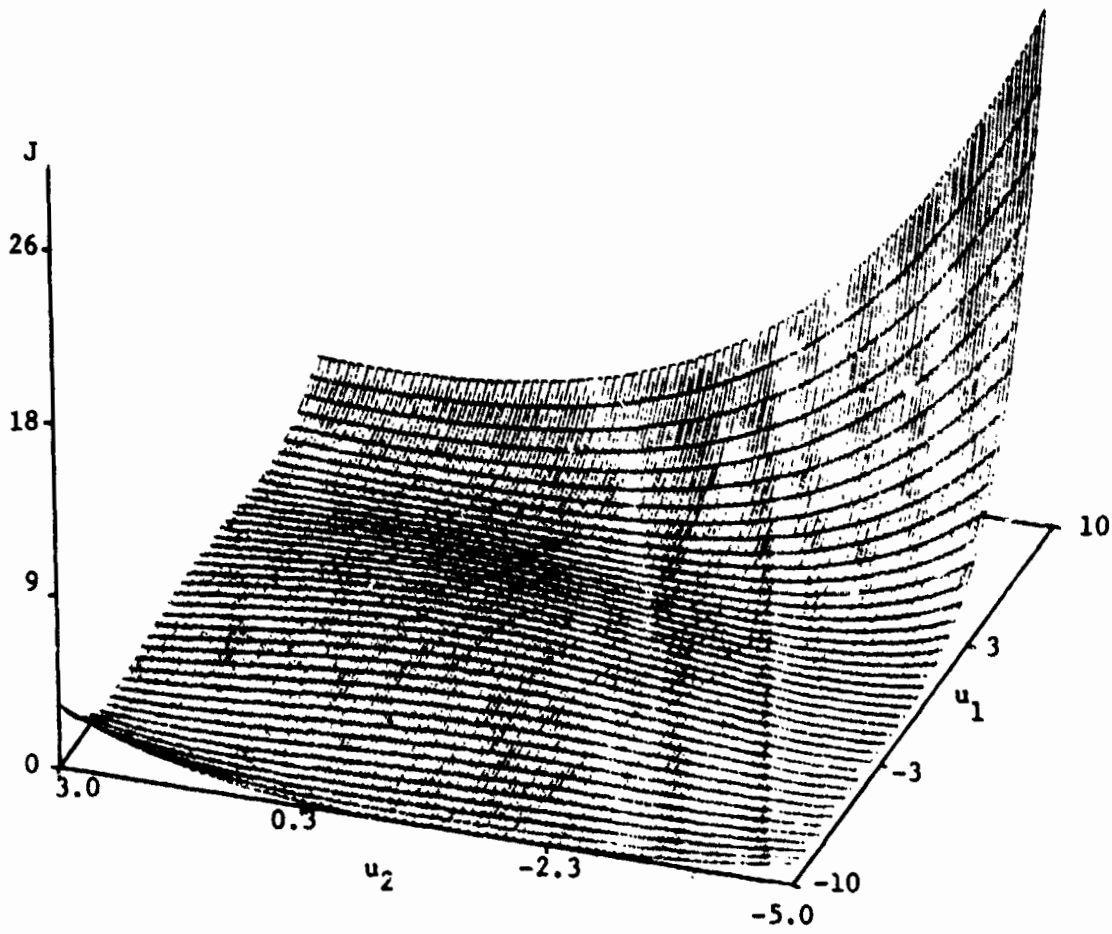

Figure 4. - Quadratic Cost Function as a Nonlinear Function of HHC u_1 and u_2 ($-10 \leq u_1 \leq +10$, $-5 \leq u_2 \leq +3$).

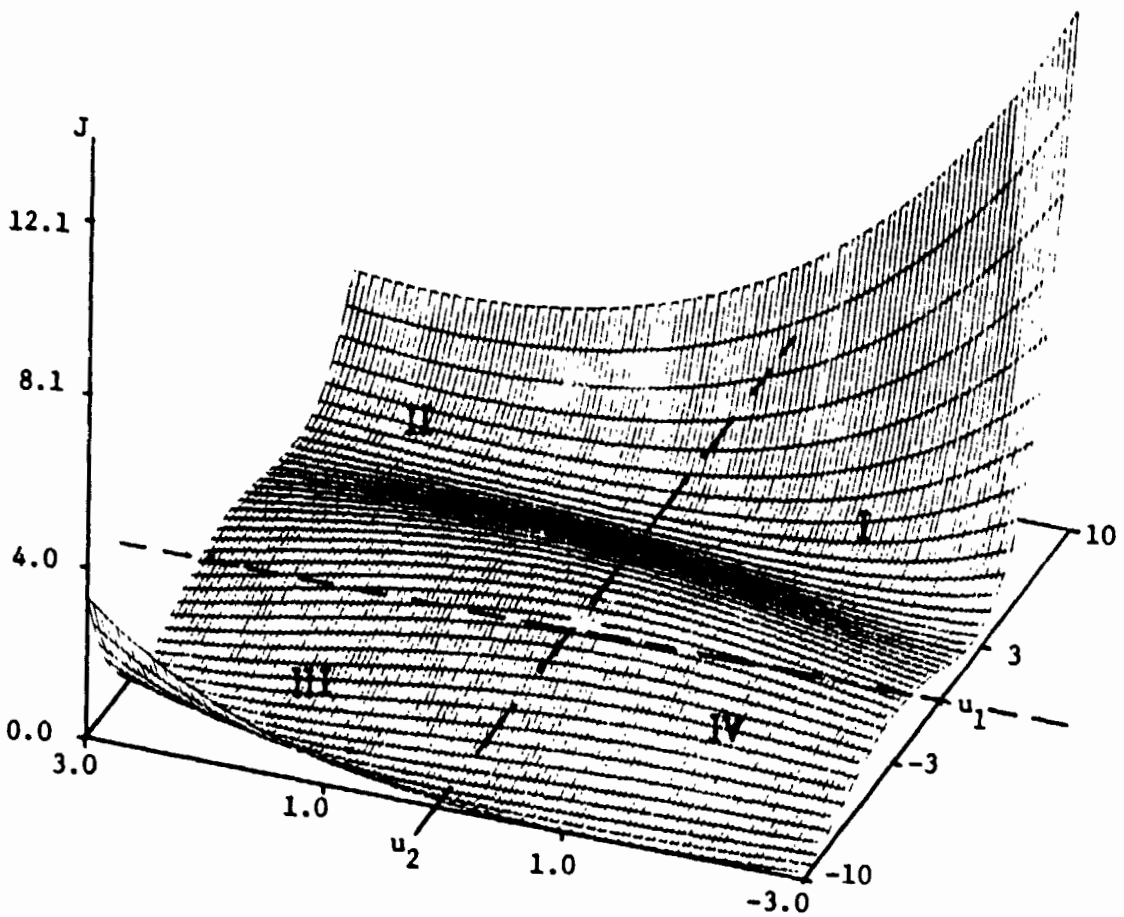

Figure 5. - Quadratic Cost Function as a Nonlinear Function of HHC u_1 and u_2 ($-10 \leq u_1 \leq +10$, $-3 \leq u_2 \leq +3$).

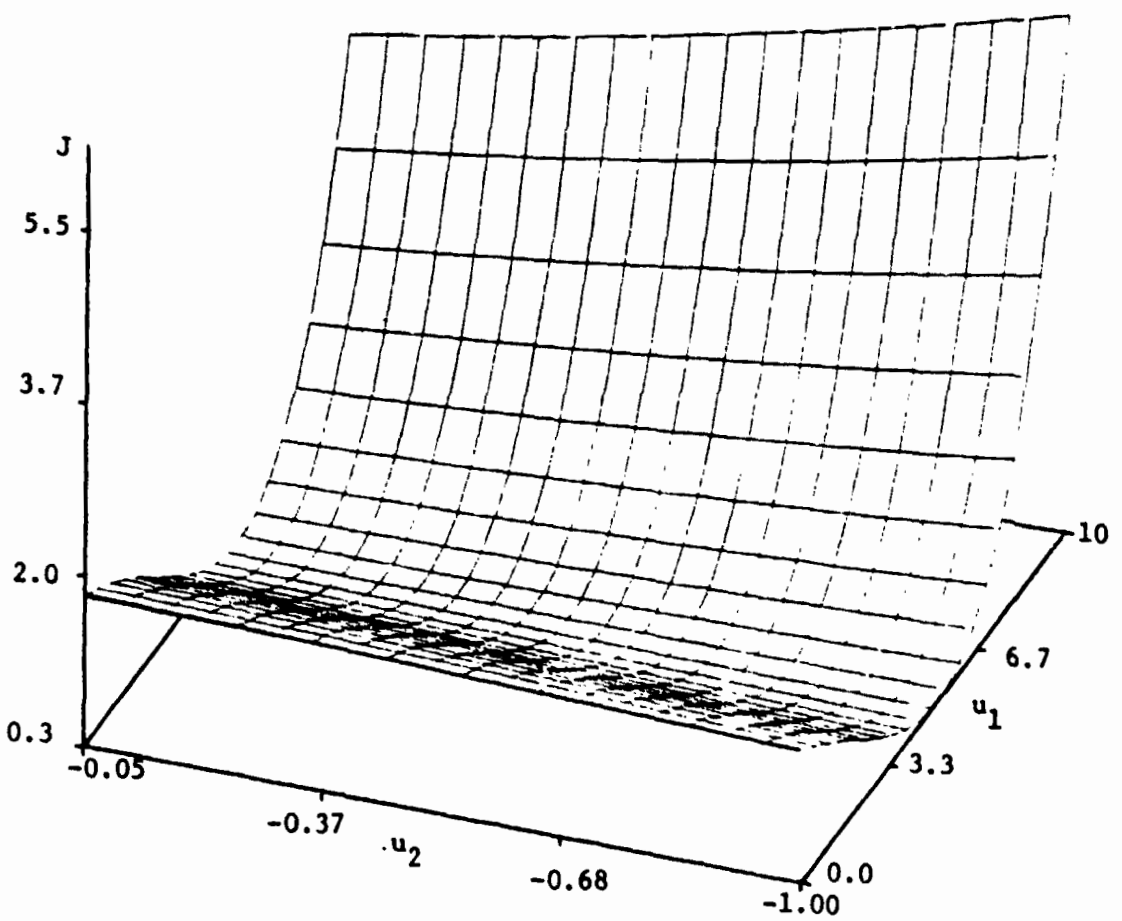

Figure 6. - Quadratic Cost Function as a Nonlinear Function of HHC u_1 and u_2 ($0 \leq u_1 \leq +10$, $0 \leq u_2 \leq -1$).

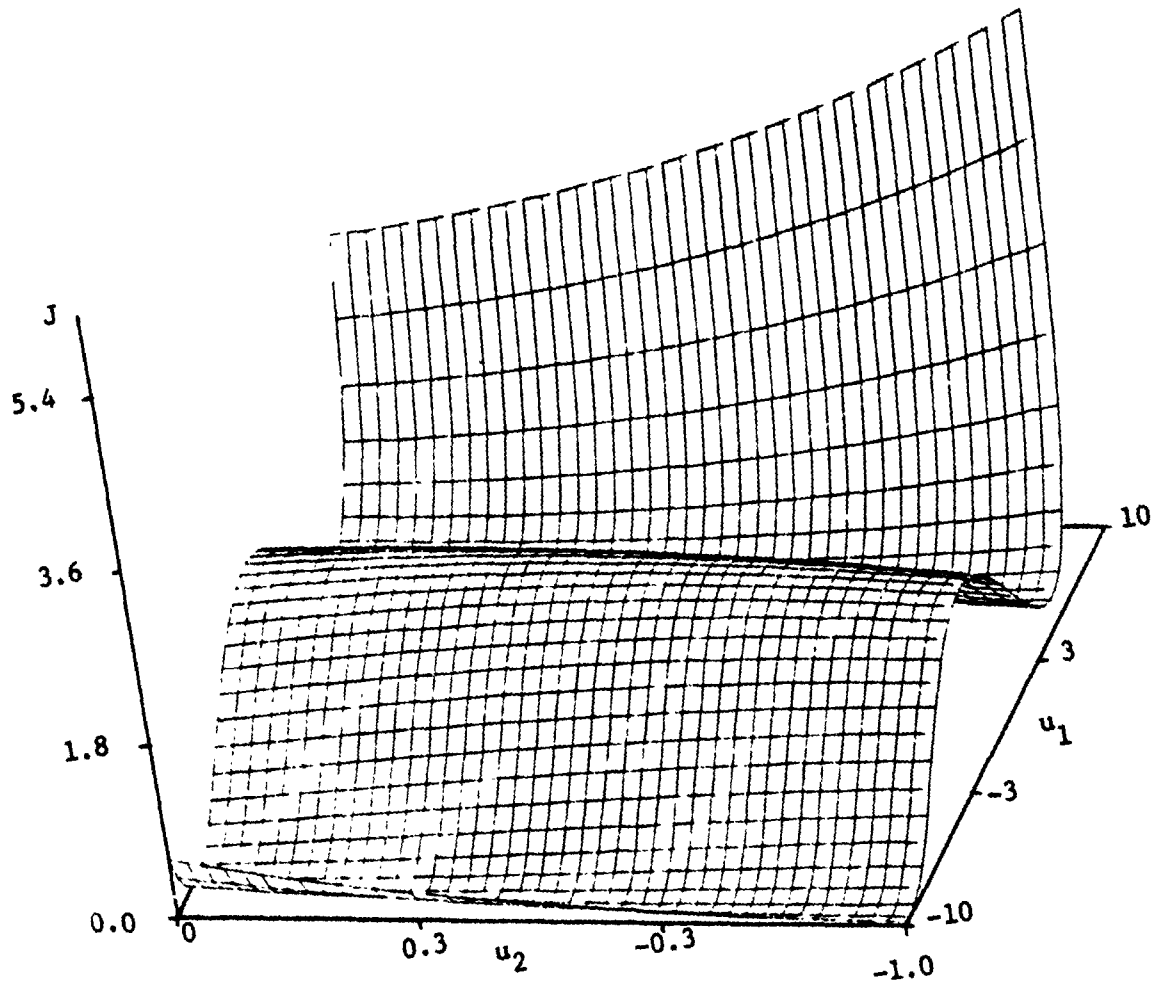

Figure 7. - Quadratic Cost Function as a Nonlinear Function of HHC u_1 and u_2 ($-10 \leq u_1 \leq +10$, $-1 \leq u_1 \leq +1$).

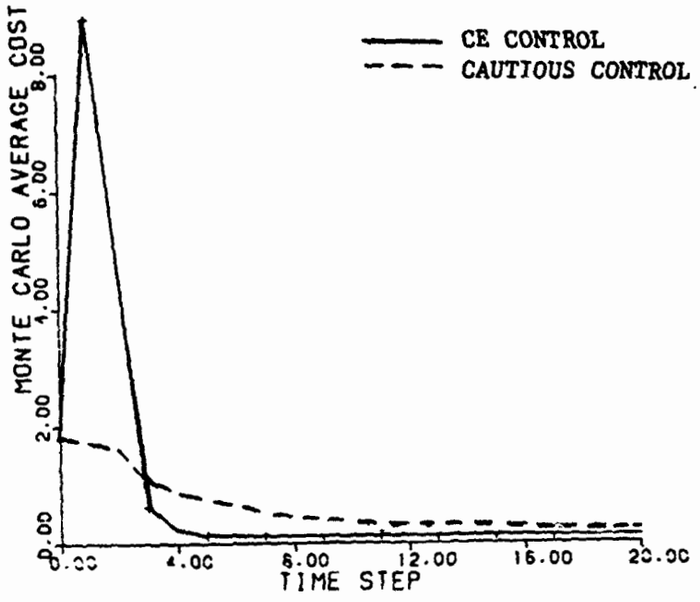

Figure 8. - Monte Carlo Average Cost (of 100 Runs) vs. Time Step Number For The Linear Vibration Model. (Global Linear Adaptive Controllers CE and Cautious).

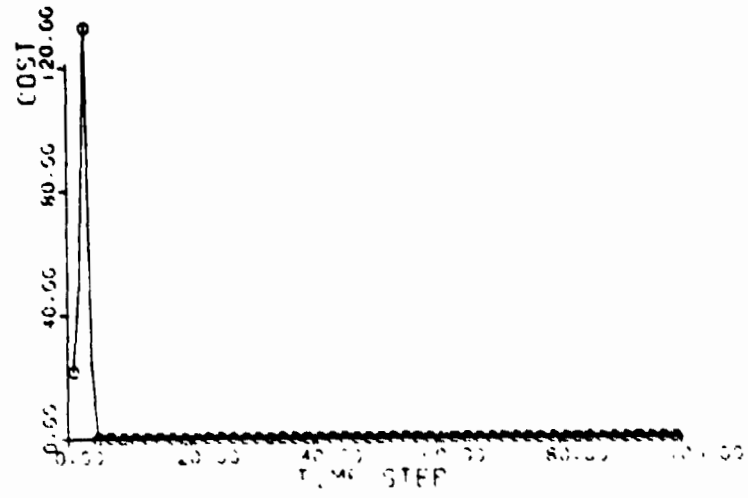

a)

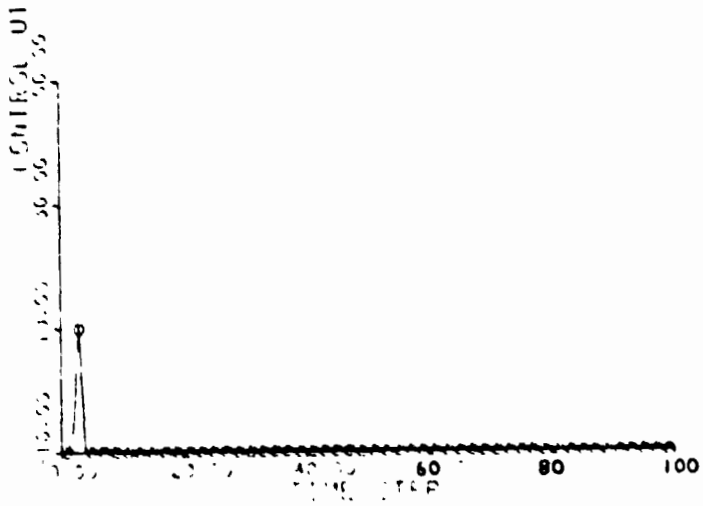

b)

Figure 9. - Convergence of the CE Global Linear Adaptive Controller on the Nonlinear Vibration Model; Cost, u_1 and u_2 vs. Time Step Number.

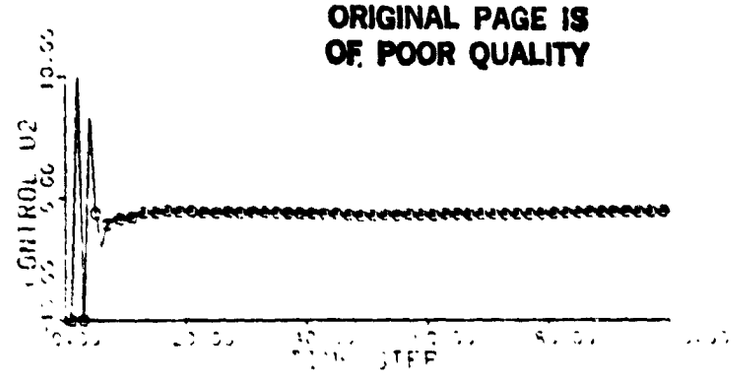

c)

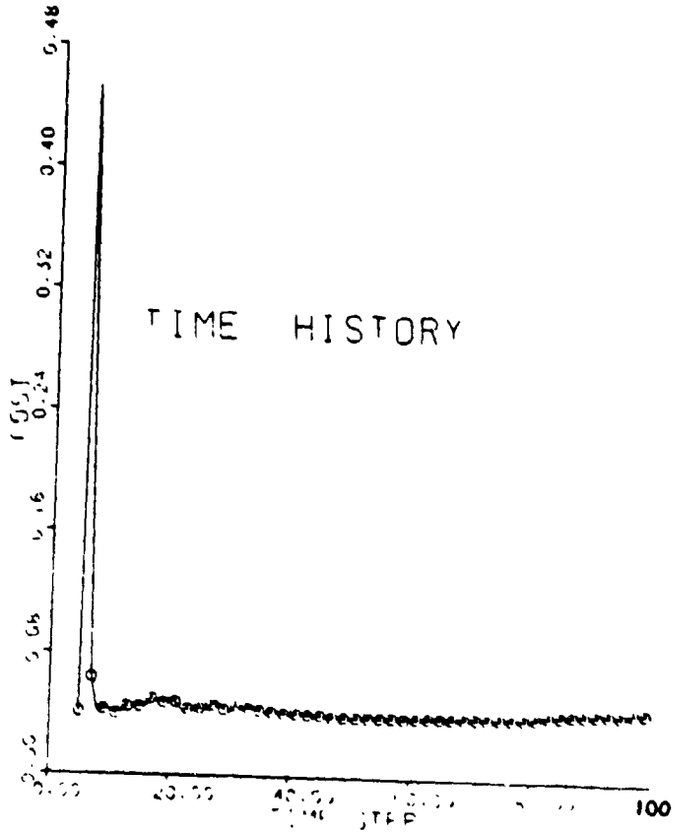

d)

Figure 9. - Concluded

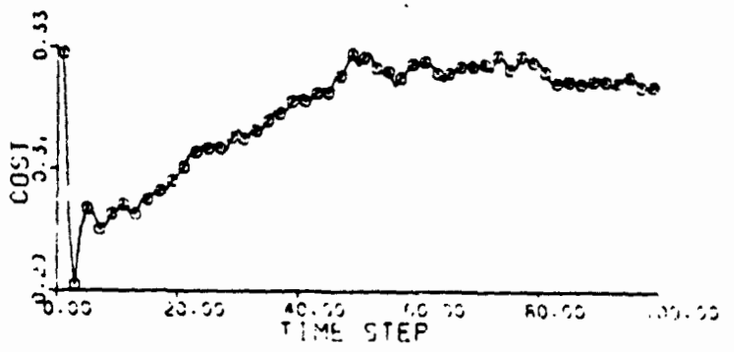

a)

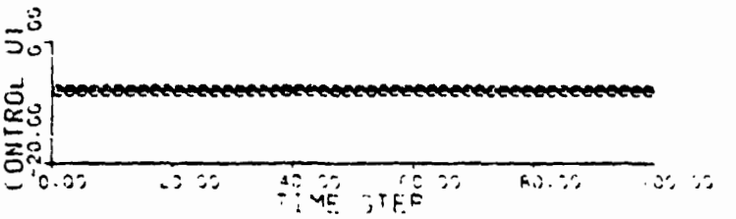

b)

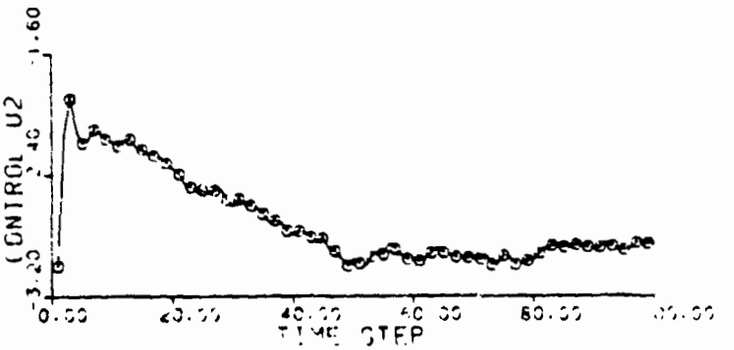

c)

Figure 10. - Convergence of the Cautious Global Linear Adaptive Controller on the Nonlinear Vibration Model; cost, u_1 and u_2 vs. Time Step. (λ = .99, P(0) x1).

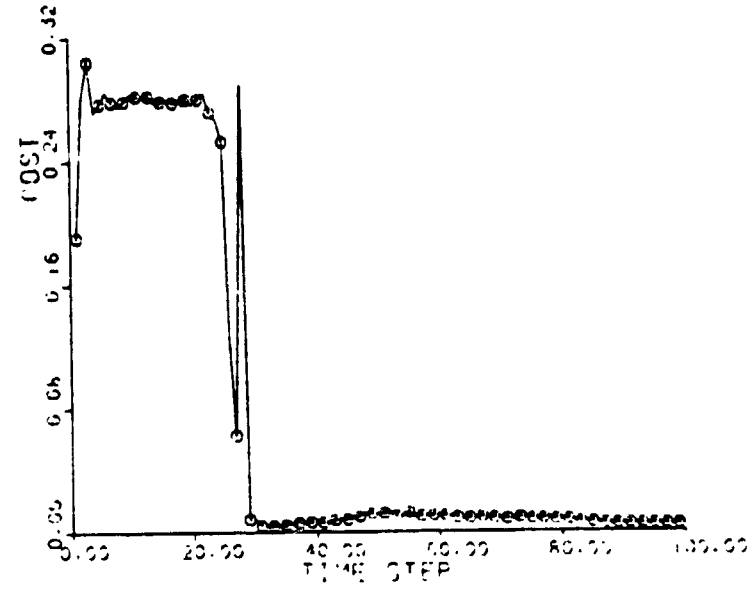

a)

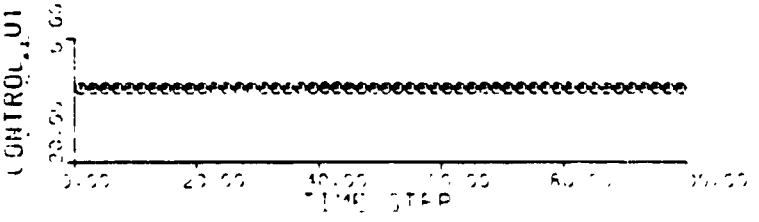

b)

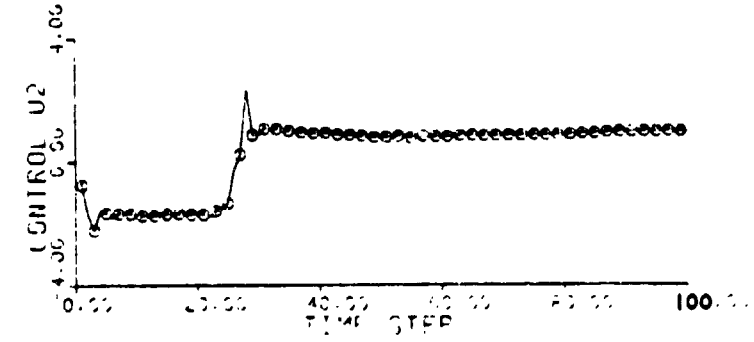

c)

Figure 11. - Convergence of the Cautious Global Linear Adaptive Controller on the Nonlinear Vibration Model; cost, u_1, and u_2 vs. Time Step. (λ = .99, P(0) x10).

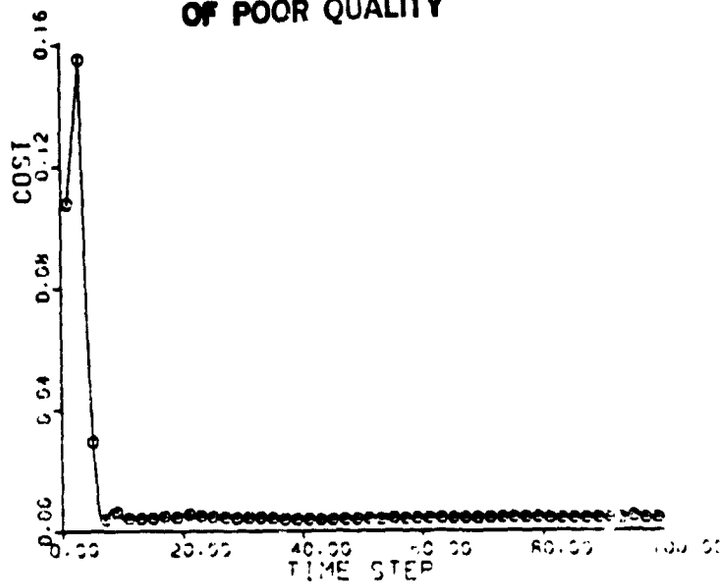

a)

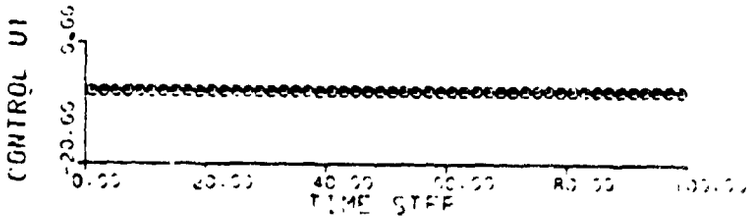

b)

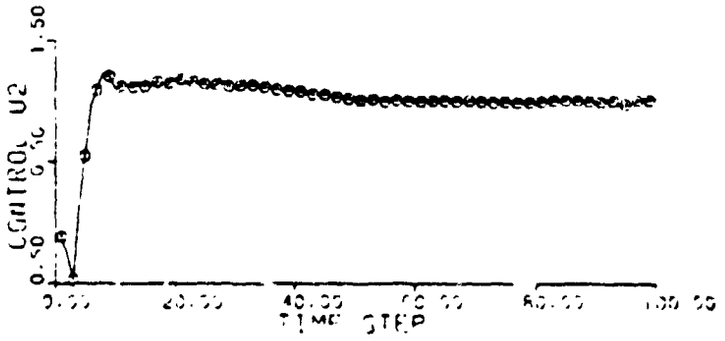

c)

Figure 12. - Convergence of the Cautious Global Linear Adaptive Controller on the Nonlinear Vibration Model; Cost, u_1, and u_2 vs. Time Step. (λ = 1, P(0) x100).

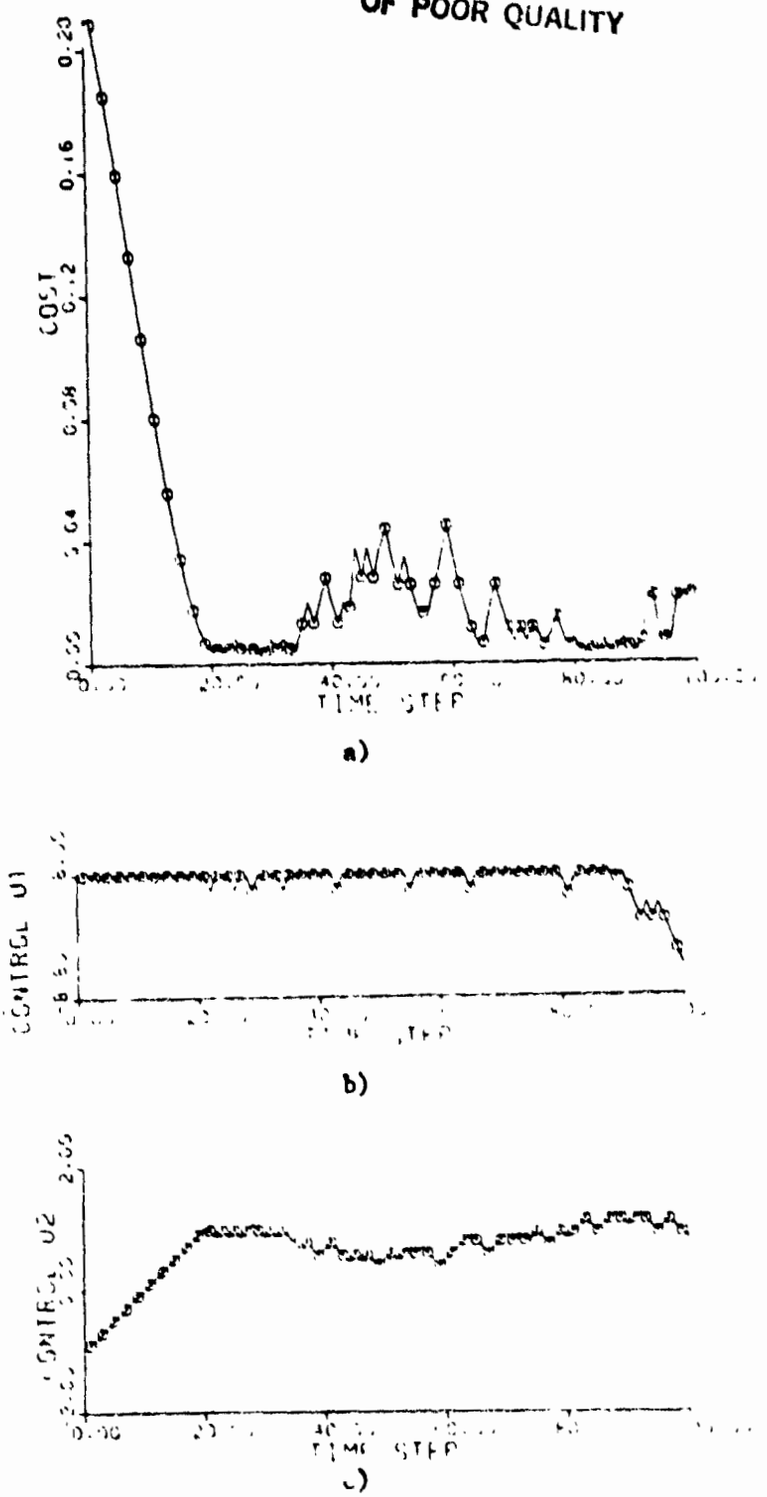

Figure 13. - Convergence of the Local Linear Adaptive Controller (CE) on the Nonlinear Vibration Model; Cost, u_1 and u_2 vs. Time Step. ($R_\Delta = 0$, $-.1 \leq \Delta u \leq .1$).

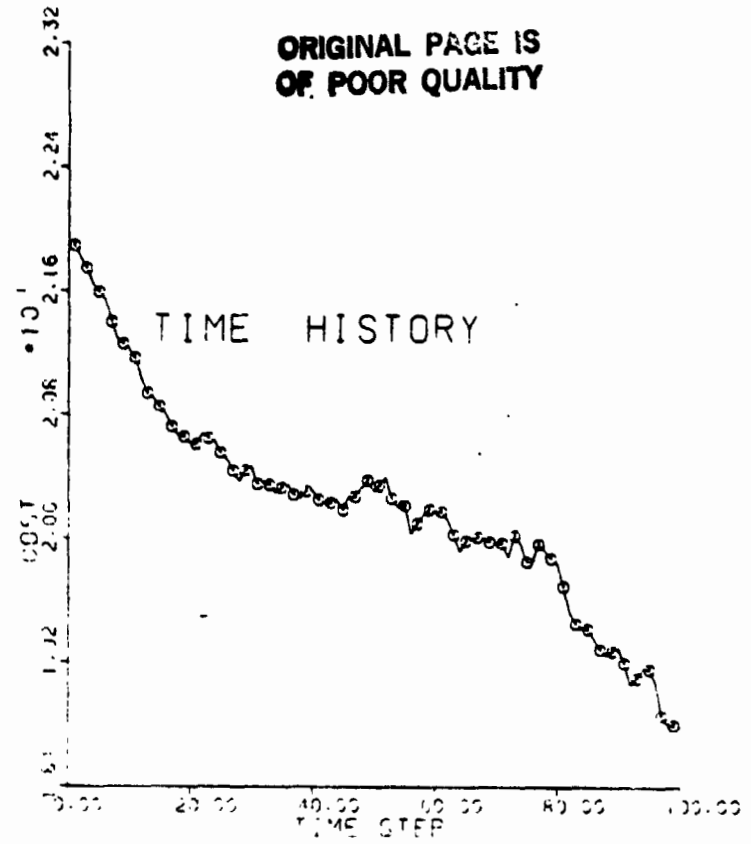

a)

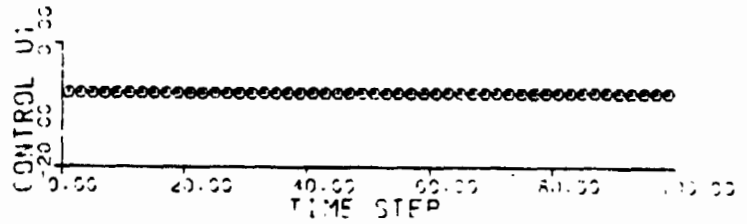

b)

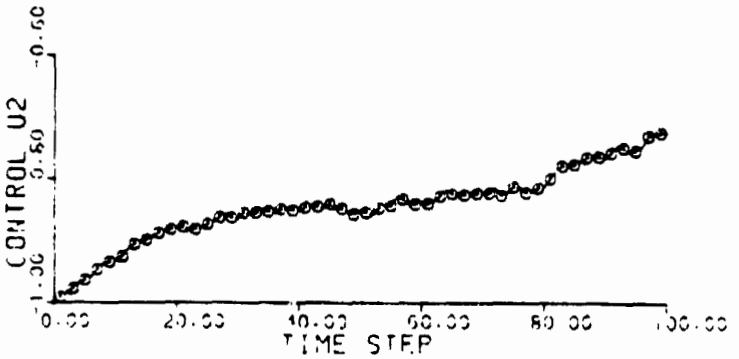

c)

Figure 14. - Convergence of the Local Linear Adaptive Controller (CE) on the Nonlinear Vibration Model; cost, u_1 and u_2 vs. Time Step. ($R_\Delta = 1$, $-.1 \leq \Delta u \leq .1$)

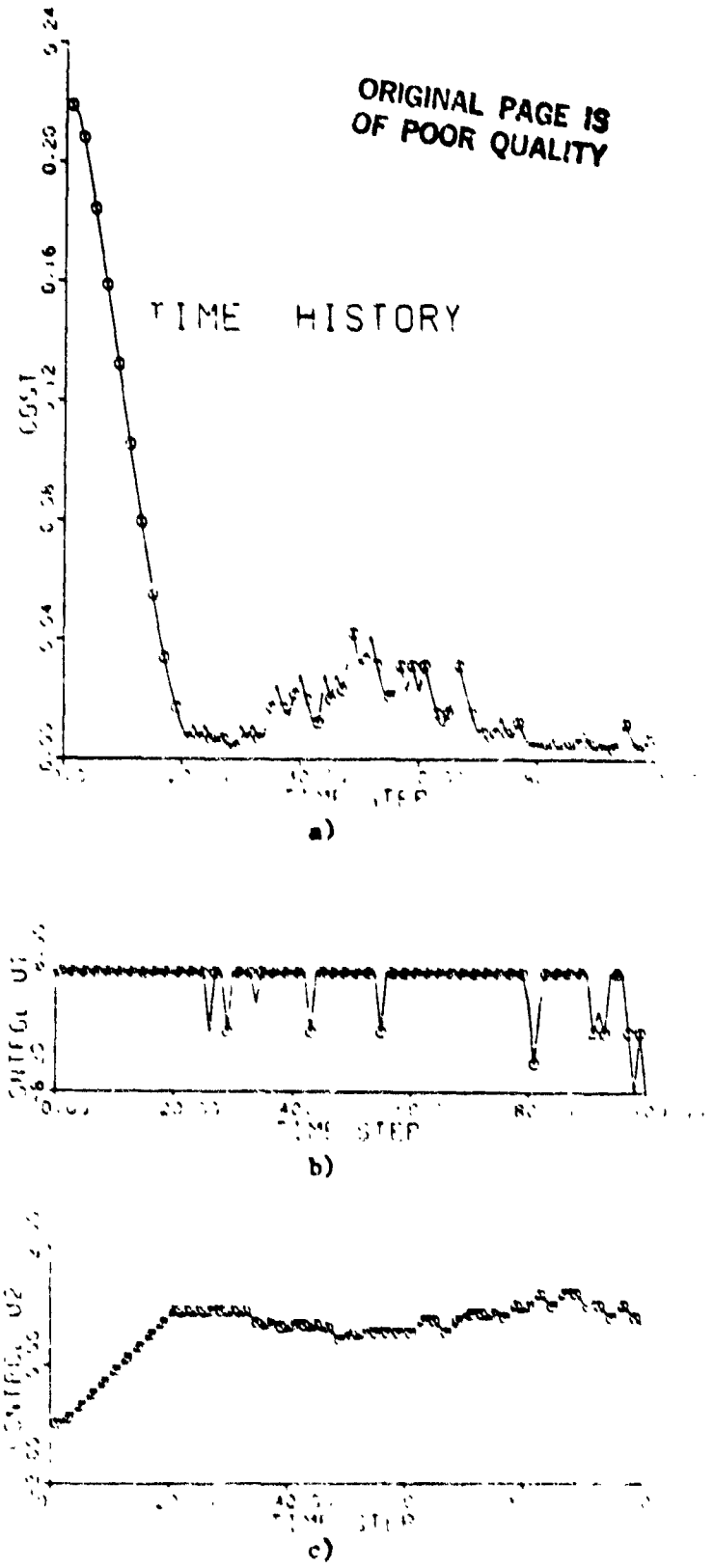

Figure 15. - Convergence of the Local Linear Adaptive Controller on the Nonlinear Vibration Model; cost, u_1 and u_2 vs. Time Step. ($R_\Delta = 1/i^2$, $-.1 \leq \Delta u \leq .1$).

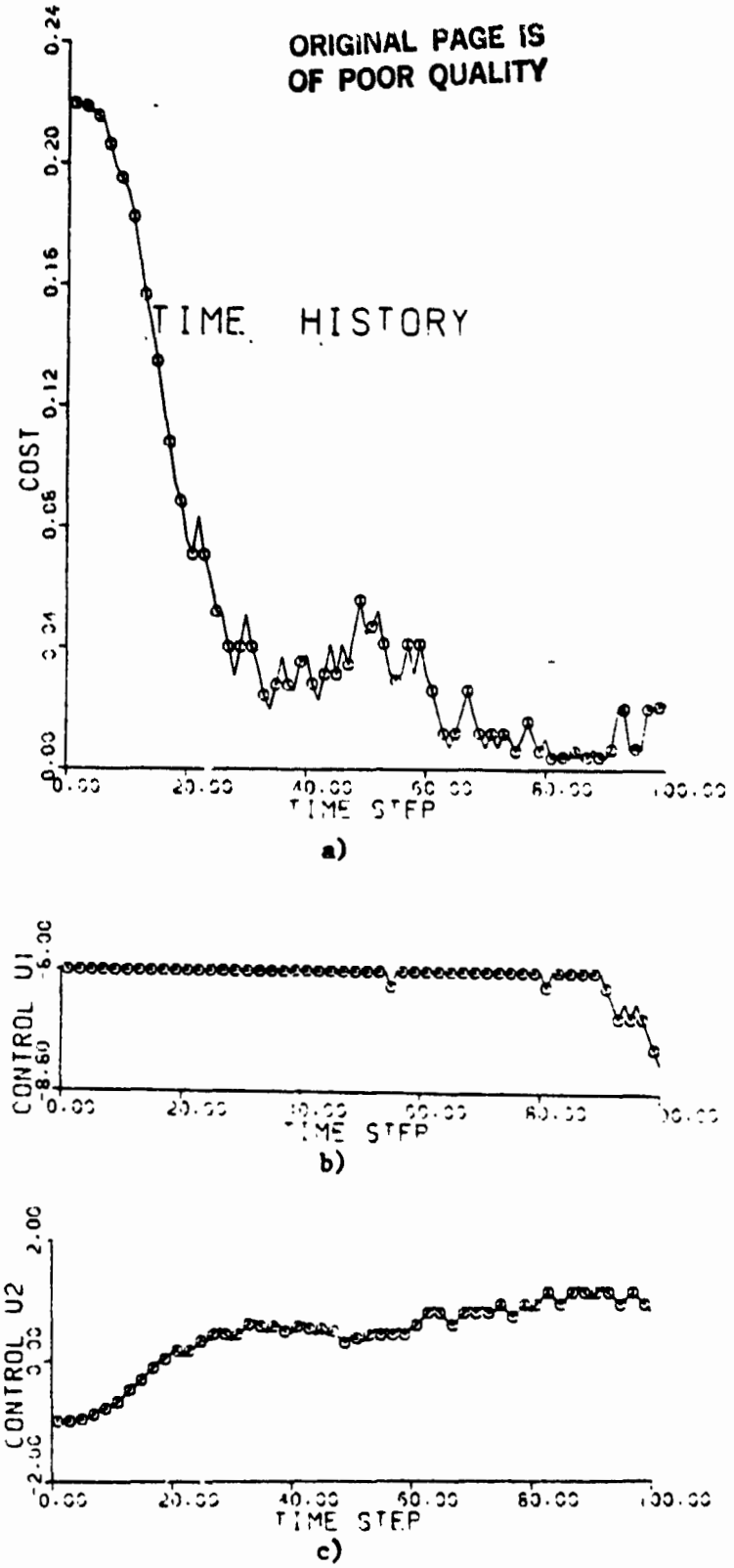

Figure 16. - Convergence of the Local LInear Adaptive Controller (CE) on the Nonlinear Vibration Model; Cost, u_1, and u_2 vs. Time Step. ($R_\Delta = 10/i^2$, $-.1 \leq \Delta u \leq .1$).

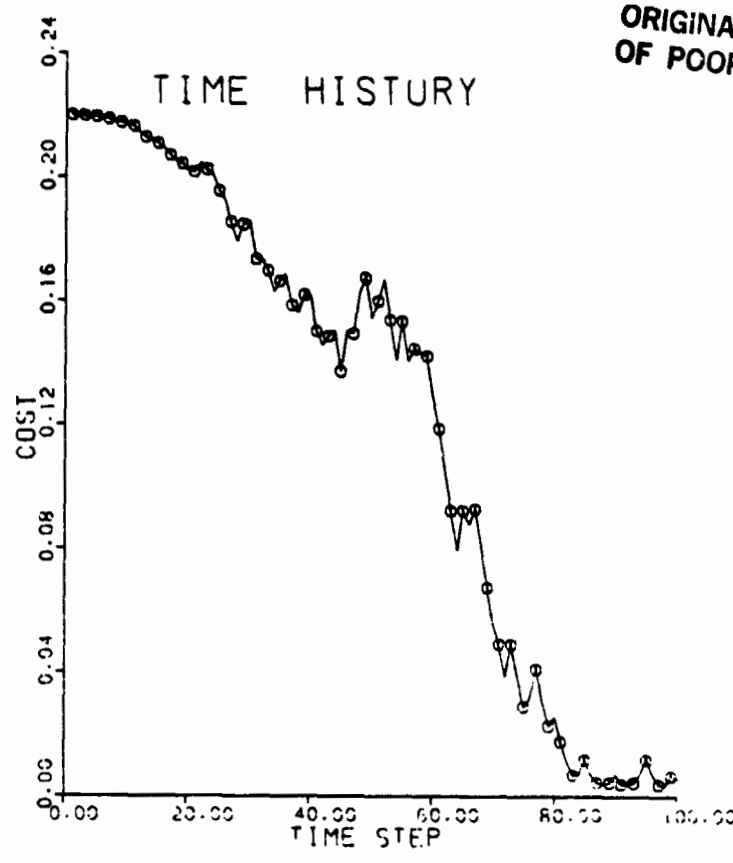

a)

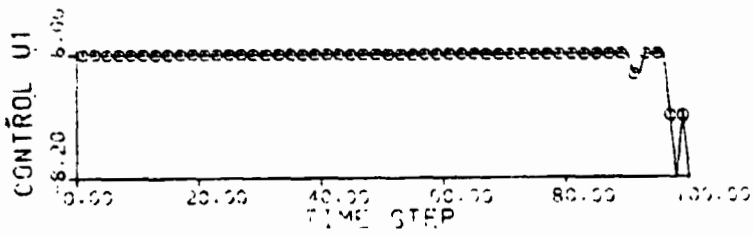

b)

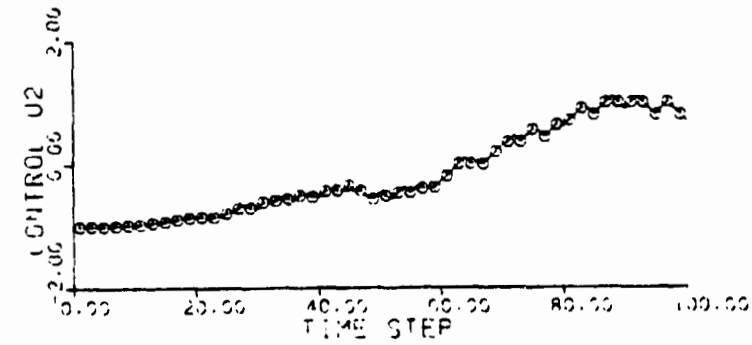

c)

Figure 17. - Convergence of the Local LInear Adaptive Controller (CE) on the Nonlinear Vibration Model; Cost, u_1, and u_2 vs. Time Step. ($R_\Delta = 100/i^2$, $-.1 \leq \Delta u \leq .1$).

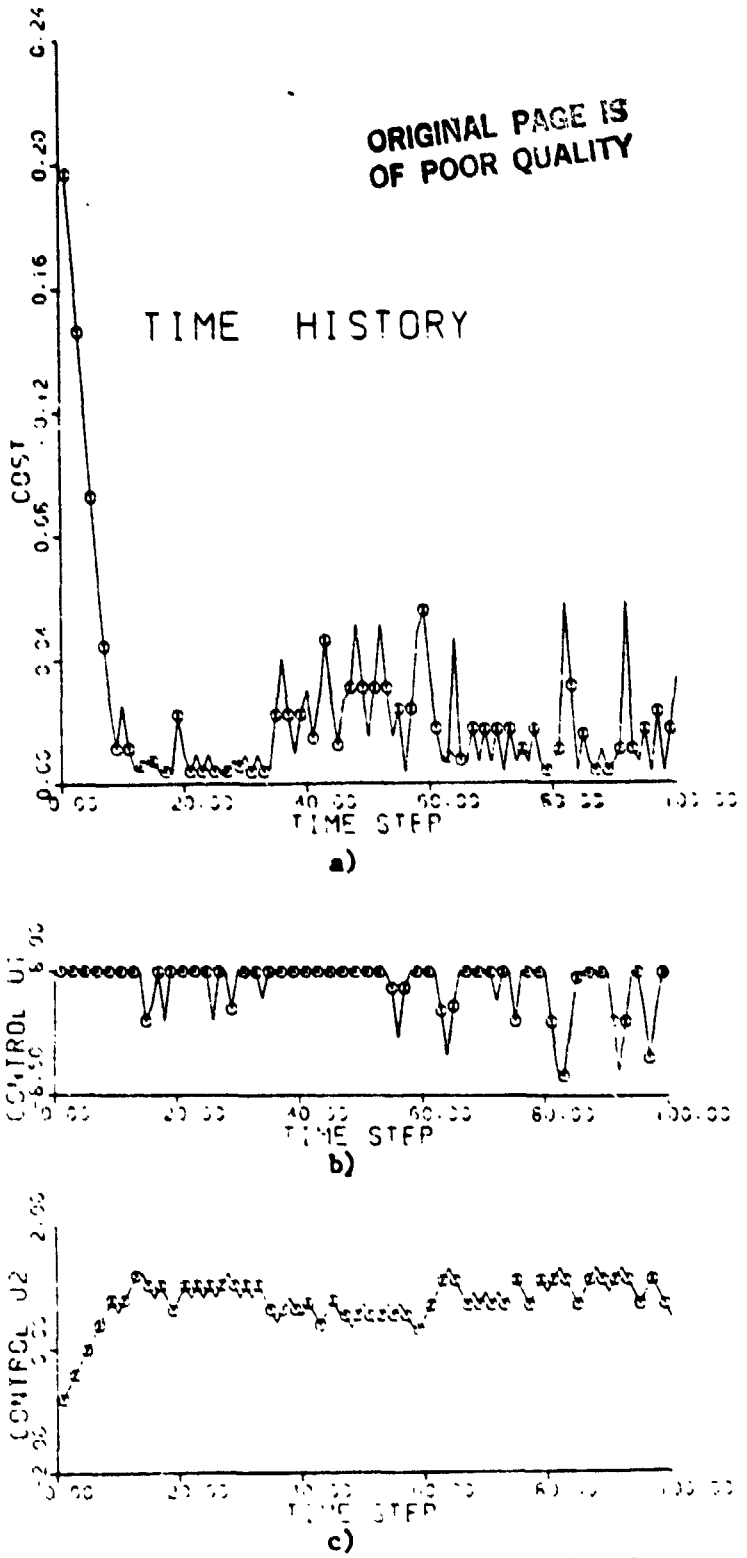

Figure 18. - Convergence of the Local Linear Adaptive Controller (CE) on the Nonlinear Vibration Simulation Model; Cost, u_1, and u_2 vs. Time Step. ($R_\Delta = 0$, $-.2 \leq \Delta u \leq .2$)

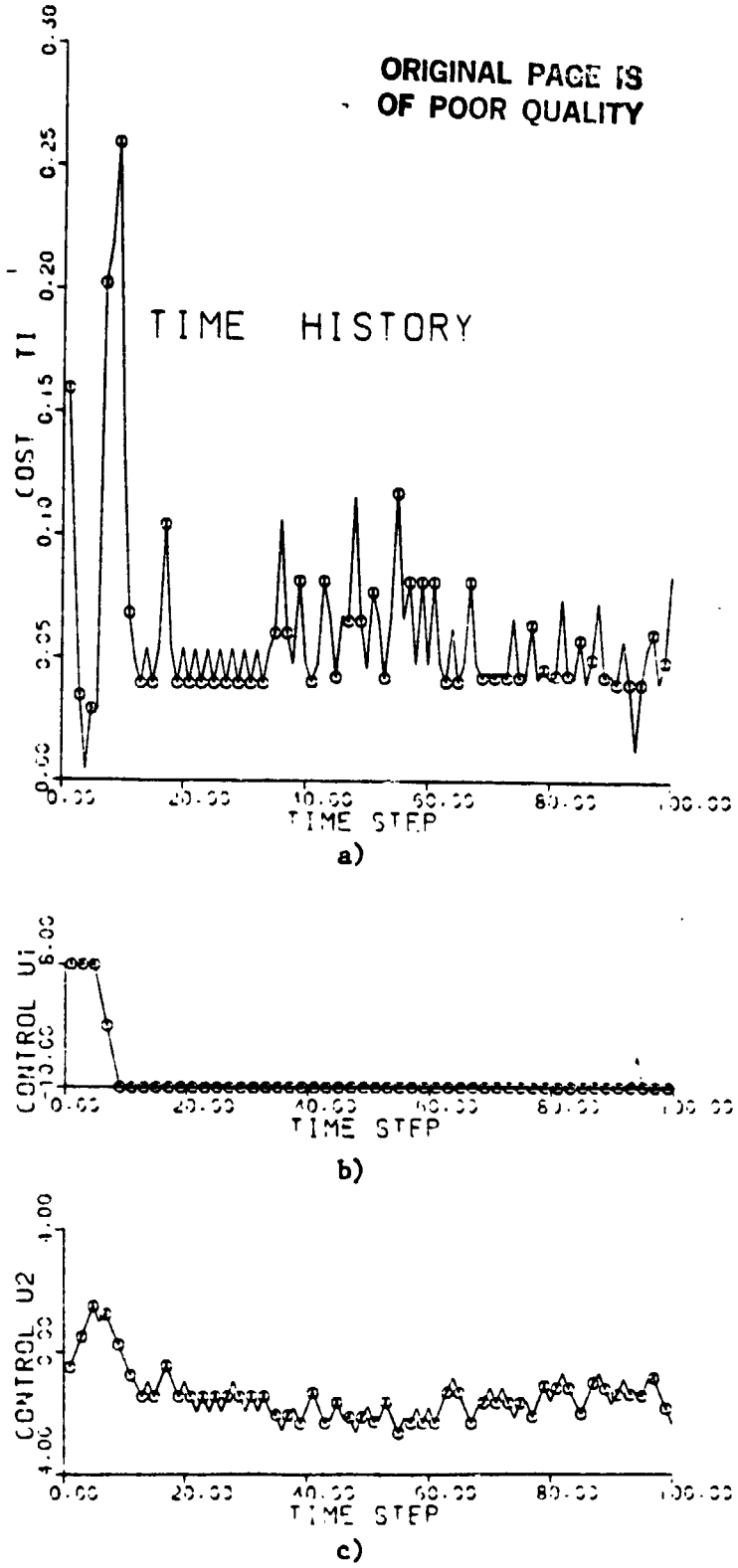

Figure 19. - Convergence of the Local Linear Adaptive Controller (CE) on the Nonlinear Vibration Simulation Model; Cost, u_1, and u_2 vs. Time Step. (R_Δ = 0, $-.5 \leq \Delta u \leq .5$)

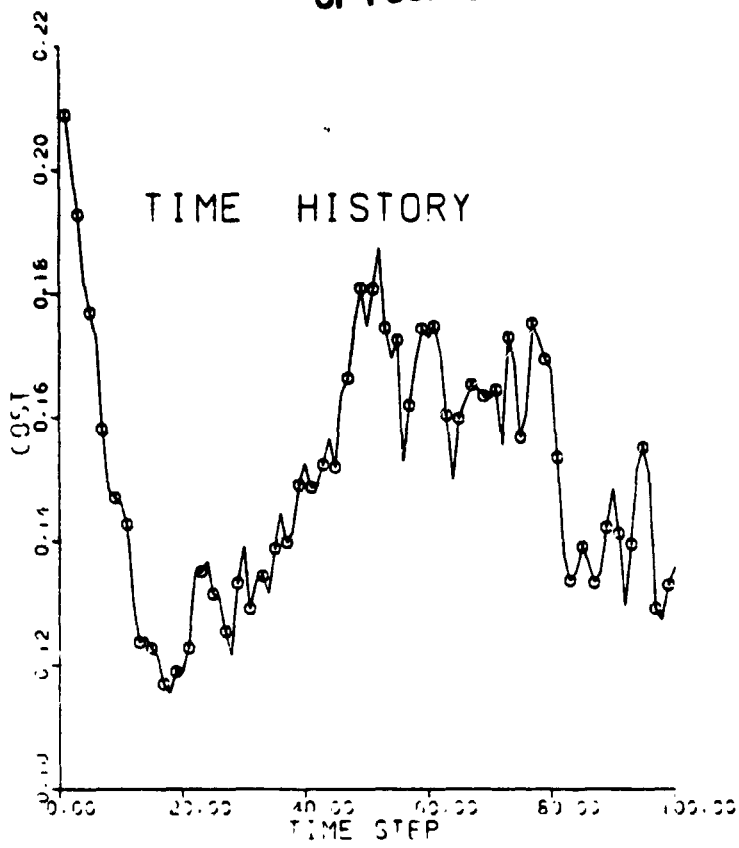

a)

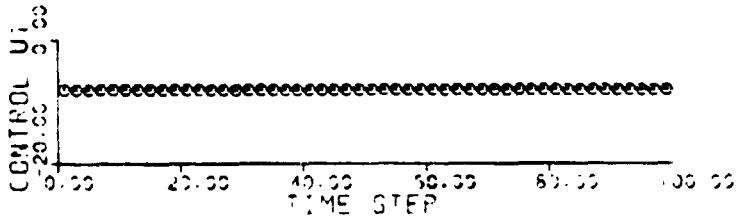

b)

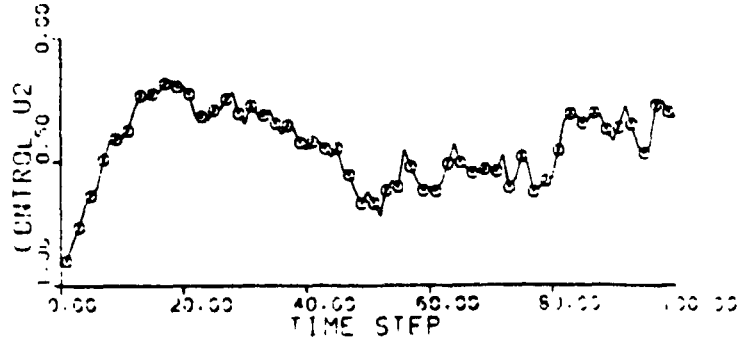

c)

Figure 20. - Convergence of the Local Linear Adaptive Controller (CE) on the Nonlinear Vibration Simulation Model; Cost, u_1, and u_2 vs. Time Step. R_Δ = .1, $-.2 \leq \Delta u \leq .2$)

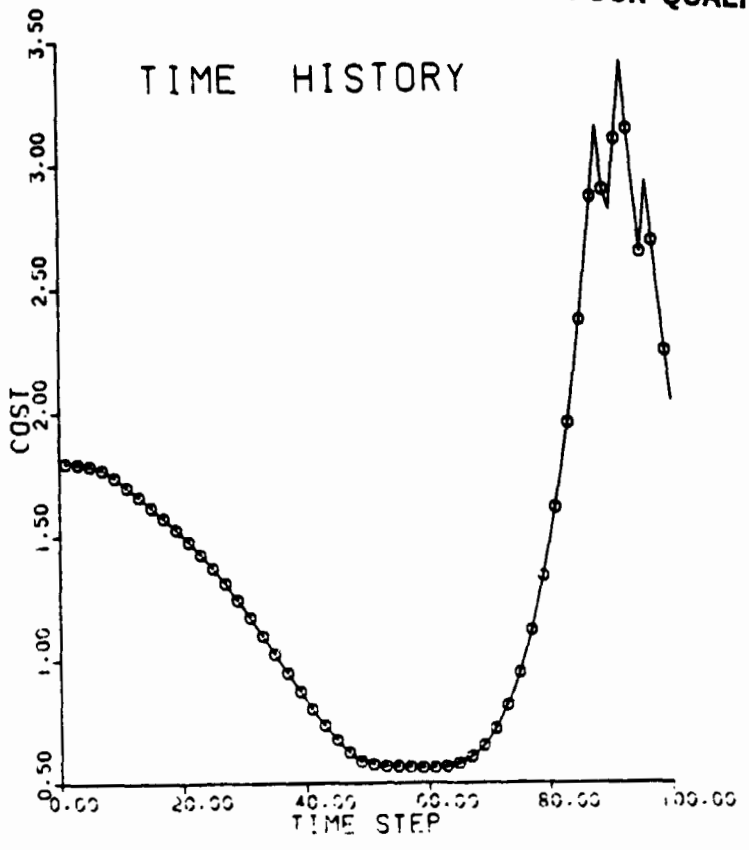

a)

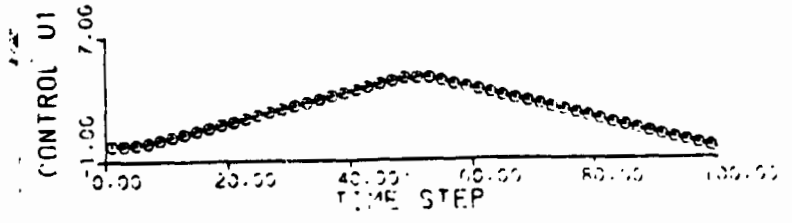

b)

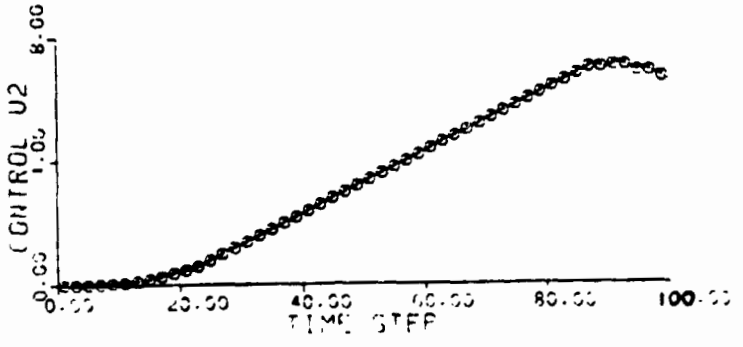

c)

Figure 21. - Divergence of Cost, u_1, and u_2 Due To Nonlinear Model Mismatch Resulting in Kalman Filter Divergence. (Local Linear Adaptive Controller, $R_\Delta = 100/i^2$, $-.1 \leq \Delta u \leq .1$, $-10 \leq u \leq +10$).